

Article

Simple One-Pot Synthesis of Hexakis(2-alkoxy-1,5-phenyleneimine) Macrocycles by Precipitation-Driven Cyclization

Toshihiko Matsumoto ^{1,2}

¹ Department of Industrial Chemistry, Graduate School of Engineering, Tokyo Polytechnic University, Atsugi 243-0297, Kanagawa, Japan; matumoto@chem.t-kougei.ac.jp or matsumoto9384@gmail.com; Tel.: +81-(0)46-270-2929 or +81-(0)178-27-7223

² National Institute of Technology, Hachinohe College, Hachinohe 039-1192, Aomori, Japan

Abstract: Hexakis(2-alkoxy-1,5-phenyleneimine) macrocycles were synthesized using a simple one-pot procedure through precipitation-driven cyclization. The acetal-protected AB-type monomers, 2-alkoxy-5-aminobenzaldehyde diethyl acetals, underwent polycondensation in water or acid-containing tetrahydrofuran. The precipitation-driven cyclization, based on imine dynamic covalent chemistry and π -stacked columnar aggregation, played a decisive role in the one-pot synthesis. The progress of the reaction was analyzed using MALDI-TOF mass spectrometry. The macrocycles with alkoxy chains were soluble in specific organic solvents, such as chloroform, allowing their structures to be analyzed using NMR. The shape-anisotropic, nearly planar, and shape-persistent macrocycles aggregated into columnar assemblies in polymerization solvents, driven by aromatic π -stacking. The octyloxy macrocycle OcO-Cm6 exhibited an enantiotropic columnar liquid crystal-like mesophase between 165 °C and 197 °C. In the SEM image of (S)-(-)-3,7-dimethyloctyloxy macrocycle (-)BCO-Cm6, columnar substances with a diameter of 200–300 nm were observed. The polymerization solution for the 2-(2-methoxyethoxy)ethoxyethoxylated macrocycle (TEGO-Cm6) gelled, and showed thixotropic properties by forming a hydrogen bond network.

Keywords: simple one-pot procedure; imine-based macrocycles; dynamic covalent polymer; Schiff base; azomethine; precipitation-driven cyclization; intra-molecular reaction; π -stacked columnar aggregates; physical gel; thixotropy



Citation: Matsumoto, T. Simple One-Pot Synthesis of Hexakis(2-alkoxy-1,5-phenyleneimine) Macrocycles by Precipitation-Driven Cyclization. *Macromol* **2024**, *4*, 1–22. <https://doi.org/10.3390/macromol4010001>

Academic Editor: Andrea Sorrentino

Received: 2 November 2023

Revised: 20 December 2023

Accepted: 27 December 2023

Published: 3 January 2024



Copyright: © 2024 by the author. Licensee MDPI, Basel, Switzerland. This article is an open access article distributed under the terms and conditions of the Creative Commons Attribution (CC BY) license (<https://creativecommons.org/licenses/by/4.0/>).

1. Introduction

Shape-persistent macrocycles are attractive in the fields of supramolecular chemistry and material science because of their unique structures and novel properties [1]. Traditionally, the extensive use of these macromolecules was impeded by laborious preparation, frequently necessitating dilute conditions, small scales, complex separations, and low overall yields. The effective production of functionalized macrocycles has been a formidable task. Over the past two decades, numerous efficient synthesis methods for shape-persistent macrocycles, via cross-coupling [2,3] or dynamic covalent chemistry (DCC) [4–9], have been developed. A dynamic covalent bond is one of the ideal linkages for the construction of large and robust organic architectures. Better results have been obtained using a dynamic covalent approach involving reversible metathesis reactions (intra-molecular reactions) that afford macrocycles in one step. Mechanistic studies demonstrate that macrocycle formation is thermodynamically controlled by the route [1]. Within the realm of macrocyclic compounds, imine macrocycles represent a significant and varied group of substances with uses in areas, such as catalysis, recognition, separation, and medical diagnostics [8–12]. Typically, imine-based macrocycles are synthesized through AA-BB type polycondensations between dialdehydes and diamines. This [n + n] condensation process can lead to the creation of a variety of macrocyclic products, such as [2 + 2], [3 + 3], and others, as well as linear oligomeric and polymeric imines. The selectivity and yields of these condensation

reactions are significantly improved when templated by transition metal ions, such as zinc (II), copper (II), or nickel (II) [13–20]. Lisowski, J. has documented that [3 + 3] macrocycles can sometimes be produced in high yields through direct condensation without the need for a metal template, specifically in the condensation of aromatic dialdehydes with chiral diamines, such as 1,2-*trans*-diaminocyclohexane [9]. The team of Lehn, J.-M. has explored the self-assembly and self-sorting behavior of dynamic covalent organic structures, enabling the simultaneous creation of multiple distinct products in a straightforward one-pot process. They have reported the self-assembly of covalent organic macrocycles and macrobicyclic cages from dialdehyde and polyamine components *via* multiple [2 + 2] and [3 + 2] polyimine condensations [13]. Imine chemistry is recognized as one of the most well-established reversible reactions and has also been a primary synthetic tool. A variety of shape-persistent macrocycles and covalent organic polyhedrons have been efficiently built in a single step through dynamic imine chemistry. Zhang, W. and co-workers have created imine-linked porous polymer networks, which demonstrate permanent porosity with high specific surface areas. Their most recent discovery is a recyclable polyimine material that can self-heal simply through heating or water treatment [21]. Zhang, D. and his team have developed covalent polymeric networks made up of imine cross-linkages, which display malleability and self-healing properties [22].

Hughes, T. and co-workers have documented the successful creation of an imine-based macrocycle from an AB-type monomer [23,24]. They crafted a unique *ortho*-phenylene-*para*-phenyleneimine macrocycle *via* a one-pot reduction and cyclooligomerization of 2-(4-nitrophenyl)benzaldehyde. Specifically, Fe(0) and aqueous HCl are used to reduce the nitroaldehyde to the AB monomer aminoaldehyde, which then spontaneously macrocyclizes to yield moderate amounts of the macrocycle. This approach is straightforward, does not require product purification, and is eco-friendly. Recently, Mori, K. and co-workers have devised a streamlined method to produce C3-symmetric imine-linked macrocycles from AB-type monomers with an aldehyde group and Boc-protected amine [25]. When the monomers were exposed to a surplus of concentrated HCl in 1,4-dioxane, the Boc group was removed, followed by a trimerization reaction *via* imine formation, leading to the successful production of the macrocycles in satisfactory chemical yields (up to 94%).

Discotic liquid crystals have disc-shaped rigid cores and flexible side chains that radiate from the core, and are also called columnar liquid crystals because they form columns by stacking. Hexakis(*m*-phenyleneimine) macrocycle Cm6, which is a disc-shaped molecule and has the property of stacking in a columnar shape [26], is expected to show a liquid crystal phase by introducing a flexible long side chain into Cm6. Tew, G. and co-workers reported that shape-persistent macrocycles with branched alkoxy- and/or tri-ethylene glycol (TEG) side chains exhibited a columnar liquid crystal phase [27]. Tanaka, K. successfully obtained a giant macrocycle with long and branched side chains, which exhibited a rectangular columnar liquid crystal phase over a wide temperature range [28]. Macrocyclic compounds can form supramolecular gels, also known as physical gels. Granata, G. and co-workers reported a supramolecular nanohydrogel formed by a bio-friendly micellar self-assembling choline-calix [4] arene derivative in the presence of curcumin, a natural and multitarget pharmacologically-relevant drug [29]. In these gels, small molecules (gelators) self-assemble through non-covalent interactions, usually into a network of fibers, to trap solvent. Many physical gels are responsive to stimuli, and often these types of gels can be reversibly converted from gel to sol (thixotropic property). These properties make them ideal candidates for investigation into a range of potential applications, including biomedical smart materials, sensors, and catalysts [30].

Our study is centered on the creation and synthesis of distinct molecular structures, such as macrocycles, using a straightforward one-pot method, and on the investigation of their unique characteristics. In our prior publication, we detailed an extremely efficient one-pot process for synthesizing a shape-persistent macrocycle, the hexakis(*m*-phenyleneimine) macrocycle Cm6, utilizing imine dynamic covalent chemistry [26].

The present article describes the synthesis of hexakis(*m*-phenyleneimine) macrocycles with long alkoxy side chains from the corresponding AB-type monomers through dynamic covalent chemistry, which includes their characterization and unique properties, such as physical gel formation.

2. Materials and Methods

2.1. Materials and Instruments

2-Hydroxy-5-nitrobenzaldehyde, platinum (IV) oxide, 5% palladium on active carbon (Pd/C), sodium hydrogen carbonate, 95% sulfuric acid, trifluoroacetic acid, dichloromethane, diethyl ether, phosphorus tribromide, and magnesium sulfate were obtained from FUJIFILM Wako Pure Chemical Co. (Wako) (Tokyo, Japan). 1-Bromooctane, (*S*)-(–)-3,7-dimethyl-6-octen-1-ol, triethoxymethane, and dichloromethane were purchased from Tokyo Chemical Industry Co., Ltd. (Tokyo, Japan). Potassium carbonate was donated by Kanto Chemical Co., Inc. (Tokyo, Japan). Tetrahydrofuran, ethanol, *N,N*-dimethylformamide (DMF), and ethyl acetate were obtained from Wako, and distilled over calcium hydride. Unless otherwise stated, all reagents were used as received without further purification.

The ^1H - and ^{13}C -NMR spectra were obtained using a JEOL JNM-LA500 spectrometer (JEOL Ltd., Tokyo, Japan). The proton signals in the ^1H -NMR spectrum were assigned from the H,H-COSY and C,H-COSY spectra. FT-IR spectra were recorded using a JASCO VALOR-III Fourier transform spectrometer (JASCO Co., Tokyo, Japan). MALDI-TOF MS measurements were conducted with an Applied Biosystems Voyager-DETEPRO-T spectrometer (Applied Biosystems, Waltham, MA, USA). 2,5-Dihydroxybenzoic acid (DHB) was used as a matrix. Middle pressure liquid chromatography (MPLC) was performed on a YAMAZEN MPLC system (YAMAZEN Co., Osaka, Japan) consisting of a YAMAZEN 540 pump, a YAMAZEN Prep UV-10V detector, and a silica gel column. TEM (JEM-2000EXII, JEOL Ltd., Tokyo, Japan) and SEM (JSM-5310, JEOL Ltd., Tokyo, Japan) were used to observe the morphology. WAXD (Rint-2000, Rigaku Co., Tokyo, Japan) was conducted using Cu-K α radiation of wavelength 1.541 Å generated at a voltage of 40 kV and a current of 30 mA. The data were acquired using a scintillation counter detector in a diffraction angle (2θ) range of 3–30° at a scanning speed of 2°/min. Thermal characterization of OcO-Cm6 and (–)BCO-Cm6 was performed with differential scanning calorimetry (DSC) using a DSC220U calorimeter from SII (SEIKO Instruments Inc., Chiba, Japan). The weight of the samples ranged from 3 to 5 mg, and the scan range was from 30 °C to 300 °C with a heating rate of 10 K/min for (–)BCO-Cm6 and 1 K/min for OcO-Cm6. Measurements using a polarizing optical microscope (POM) were carried out with an OLYMPUS DP70 polarizing microscope (OLYMPUS Co., Tokyo, Japan), equipped with a METTLER-TOLEDO FP82HT hot stage (METTLER-TOLEDO Co., Tokyo, Japan). Circular dichroism (CD) spectra were measured in chloroform at a concentration of 0.1 mmol/L. Spectra were recorded with a JASCO J820 spectropolarimeter (JASCO Co., Tokyo, Japan) in the 200–700 nm range (100 nm/min, 2 nm slit width) in a 10 mm path-length quartz cell. The baseline spectrum was recorded from pure chloroform.

2.2. Preparation of Monomers

2.2.1. 2-Alkoxy-5-nitrobenzaldehydes

Three types of 2-alkoxy-5-nitrobenzaldehydes, including 2-octyloxy-5-nitrobenzaldehyde, 2-(*S*)-(–)-3,7-dimethyloctyloxy-5-nitrobenzaldehyde, and 2-(2-(2-(2-methoxyethoxy)ethoxy)ethoxy)-5-nitrobenzaldehyde, were prepared from 2-hydroxy-5-nitrobenzaldehyde and the corresponding 1-bromoalkanes, according to the Williamson ether synthesis [31]. A representative procedure for 2-octyloxy-5-nitrobenzaldehyde is as follows: In a 300 mL flask with an Allihn condenser, 2-hydroxy-5-nitrobenzaldehyde (4.01 g, 23.0 mmol), potassium carbonate (5.05 g, 36.0 mmol), and DMF (solvent, 100 mL) were placed. 1-Bromooctane (5.07 g, 26.0 mmol) was added dropwise to the solution, and then it was refluxed at 100 °C for 60 h. The product was extracted with dichloromethane and the extract was dried over magnesium sulfate and then concentrated by evaporation to give

2-octyloxy-5-nitrobenzaldehyde. The other 2-alkoxy-5-nitrobenzaldehydes were synthesized according to a similar procedure as mentioned above, except that 1-bromooctane was replaced by (S)-(-)-1-bromo-3,7-dimethyloctane for 2-(S)-(-)-(3,7-dimethyloctyloxy)-5-nitrobenzaldehyde, and by 1-bromo-2-(2-(2-methoxyethoxy)ethoxy)ethane for 2-(2-(2-(2-methoxyethoxy)ethoxy)ethoxy)-5-nitrobenzaldehyde. (S)-(-)-1-Bromo-3,7-dimethyloctane and 1-bromo-2-(2-(2-methoxyethoxy)ethoxy)ethane were prepared by the bromination of (S)-(-)-3,7-dimethyloctanol and triethylene glycol monomethyl ether with phosphorus tribromide, respectively. 2-(S)-(-)-(3,7-Dimethyloctyloxy)-5-nitrobenzaldehyde and 2-(2-(2-(2-methoxyethoxy)ethoxy)ethoxy)-5-nitrobenzaldehyde were purified with YAMAZEN Automated Flash Chromatograph (YAMAZEN Co., Osaka, Japan). Experimental procedures of (S)-(-)-1-bromo-3,7-dimethyloctane, 1-bromo-2-(2-(2-methoxyethoxy)ethoxy)ethane, and the NMR spectra were described in the Supplementary Materials (Experimental procedures and Figures S1–S6).

2-Octyloxy-5-nitrobenzaldehyde: Yield 87%. $^1\text{H-NMR}$ (CDCl_3 , δ): 0.89 (t, $J = 6.1$ Hz, 3H, H-d), 1.30 (m, 8H), 1.51 (quin, $J = 7.7$ Hz, 2H, H-c), 1.91 (quin, $J = 6.7$ Hz, 2H, H-b), 4.22 (t, $J = 6.4$ Hz, 2H, H-a), 7.10 (d, $J = 9.2$ Hz, 1H, H-5), 8.41 (quar, $J = 6.1$ Hz, 1H, H-4), 8.69 (d, $J = 2.8$ Hz, 1H, H-2), 10.48 (s, 1H, CHO). $^{13}\text{C-NMR}$ (CDCl_3 , δ): 14.1 (C-b), 28.9, 29.16, 29.23, 31.8, 69.9 (C-a), 112.9 (C-5), 124.5 (C-2), 124.7 (C-4), 130.6 (C-1), 141.5 (C-3), 165.3 (C-6), 187.6 (CHO). (Figures S7 and S8).

2-(S)-(-)-(3,7-Dimethyloctyloxy)-5-nitrobenzaldehyde: Yield 81%. $^1\text{H-NMR}$ (CDCl_3 , δ): 0.87 (d, $J = 6.7$ Hz, 6H), 1.00 (d, $J = 6.1$ Hz, 3H), 1.14–1.39 (m, 6H), 1.49–1.57 (m, 1H), 1.93–1.99 (m, 2H), 4.25–4.32 (m, 2H), 7.15 (d, $J = 9.1$ Hz, 1H), 8.40 (d, $J = 9.4$ Hz, 1H), 8.64 (d, $J = 2.7$ Hz, 1H), 10.45 (s, 1H, CHO). $^{13}\text{C-NMR}$ (CDCl_3 , δ): 19.6, 22.6, 22.7, 24.7, 28.0, 29.9, 35.7, 37.2, 39.2, 68.4, 113.1, 124.3, 124.6, 130.6, 141.4, 165.3, 187.5. (Figures S9–S15).

2-(2-(2-(2-Methoxyethoxy)ethoxy)ethoxy)-5-nitrobenzaldehyde: Yield 87%. $^1\text{H-NMR}$ (CDCl_3 , δ): 3.37 (s, 3H, H-14), 3.53–3.55 (m, 2H, H-13), 3.63–3.69 (m, 4H, H-11,12), 3.74–3.77 (m, 2H, H-10), 3.98 (t, $J = 4.5$, 2H, H-9), 4.42 (t, $J = 4.5$ Hz, 2H, H-8), 7.19 (d, $J = 9.4$ Hz, 1H, H-5), 8.41 (d, $J = 6.4$ Hz, 1H, H-4), 8.66 (d, $J = 2.7$ Hz, 1H, H-2), 10.48 (s, 1H, H-7). $^{13}\text{C-NMR}$ (CDCl_3 , δ): 59.0 (C-14), 69.2 (C-8(9)), 69.4 (C-9(8)), 70.60 (C-10(11 or 12)), 70.64 (C-11(10 or 12)), 71.0 (C-12(10 or 11)), 71.9 (C-13), 113.5 (C-5), 124.3 (C-2), 124.8 (C-1), 130.5 (C-4), 141.7 (C-3), 165.1 (C-6), 187.6 (C-7). (Figures S16–S21).

2.2.2. 2-Alkoxy-5-nitrobenzaldehyde Diethyl Acetals

2-Alkoxy-5-nitrobenzaldehyde diethyl acetals were synthesized by acid-catalyzed acetalation from the corresponding aldehydes. A representative procedure for 2-octyloxy-5-nitrobenzaldehyde diethyl acetal is as follows: In a 200 mL flask equipped with an Allihn condenser, a mixture of 2-octyloxy-5-nitrobenzaldehyde (5.86 g, 20 mmol), triethoxymethane (4.65 g, 31 mmol), ethanol (as a solvent, 100 mL), and sulfuric acid (50 μL) was prepared and subjected to reflux for 60 h. The reaction mixture was neutralized with saturated NaHCO_3 aq. solution, the product was extracted with dichloromethane, and the extract was dried over magnesium sulfate then concentrated by evaporation. The other 2-alkoxy-5-nitrobenzaldehydes were synthesized according to a similar procedure as mentioned above, except that 2-octyloxy-5-nitrobenzaldehyde was replaced by 2-(S)-(-)-(3,7-dimethyloctyloxy)-5-nitrobenzaldehyde for 2-(S)-(-)-(3,7-dimethyloctyloxy)-5-nitrobenzaldehyde diethyl acetal, and by 2-(2-(2-(2-methoxyethoxy)ethoxy)ethoxy)-5-nitrobenzaldehyde for 2-(2-(2-(2-methoxyethoxy)ethoxy)ethoxy)-5-nitrobenzaldehyde diethyl acetal.

2-Octyloxy-5-nitrobenzaldehyde diethyl acetal: Yield 80%. $^1\text{H-NMR}$ (CDCl_3 , δ): 0.89 (t, $J = 6.7$ Hz, 3H, H-e), 1.25 (t, $J = 7.0$ Hz, 6H, H-d), 1.29 (m, 8H), 1.49 (quin, $J = 7.6$ Hz, 2H), 1.85 (quin, $J = 7.0$ Hz, 2H), 3.63 (m, 4H, H-c), 4.10 (t, $J = 6.4$ Hz, 2H, H-b), 5.72 (s, 1H, -CH(acetal)), 6.91 (d, $J = 8.9$ Hz, 1H, H-5), 8.18 (quar, $J = 6.1$ Hz, 1H, H-4), 8.47 (d, $J = 2.8$ Hz, 1H, H-2). $^{13}\text{C-NMR}$ (CDCl_3 , δ): 14.1 (C-e), 15.2 (C-d), 29.0, 29.23, 29.27, 31.8, 62.6 (C-c), 69.1 (C-b), 96.7 (C-a), 111.1 (C-5), 123.6 (C-2), 125.8 (C-4), 128.7 (C-1), 141.2 (C-3), 161.5 (C-6). (Figures S22 and S23).

2-(S)-(-)-(3,7-dimethyloctyloxy)-5-nitrobenzaldehyde diethyl acetal: Yield 92%. $^1\text{H-NMR}$ (CDCl_3 , δ): 0.87 (d, $J = 6.7$ Hz, 6H), 0.96 (d, $J = 6.4$ Hz, 3H), 1.14–1.36 (m, 6H), 1.24 (t, $J = 7.0$ Hz, 6H), 1.49–1.73 (m, 3H), 1.86–1.92 (m, 1H), 3.56–3.71 (m, 4H), 4.11–4.15 (m, 2H), 6.93 (d, $J = 9.1$ Hz, 1H), 8.19 (d, $J = 9.1$ Hz, 1H), 8.48 (d, $J = 2.7$ Hz, 1H). $^{13}\text{C-NMR}$ (CDCl_3 , δ): 15.2, 19.6, 22.6, 22.7, 24.7, 28.0, 29.8, 36.0, 37.2, 39.2, 62.6, 67.5, 96.7, 111.0, 123.6, 125.8, 128.7, 141.2, 161.4. (Figures S24 and S25).

2-(2-(2-(2-Methoxyethoxy)ethoxy)ethoxy)-5-nitrobenzaldehyde diethyl acetal: Yield 92%. $^1\text{H-NMR}$ (CDCl_3 , δ): 1.21 (t, $J = 7.0$ Hz, 6H), 3.37 (s, 3H), 3.53–3.55 (m, 2H), 3.59–3.71 (m, 8H), 3.73–3.74 (m, 2H), 3.91 (t, $J = 4.8$ Hz, 2H), 4.28 (t, $J = 4.5$ Hz, 2H), 5.74 (s, 1H), 6.98 (d, $J = 9.1$ Hz, 1H), 8.10 (d, $J = 6.1$ Hz, 1H), 8.47 (d, $J = 3.0$ Hz, 1H). $^{13}\text{C-NMR}$ (CDCl_3 , δ): 15.2, 59.0, 62.7, 68.7, 69.4, 70.6, 70.7, 70.9, 72.0, 96.6, 111.6, 123.6, 125.6, 129.1, 141.5, 161.2. (Figures S26 and S27).

2.2.3. 2-Alkoxy-5-aminobenzaldehyde Diethyl Acetals

2-Alkoxy-5-aminobenzaldehyde diethyl acetals were prepared by catalytic hydrogenation of the corresponding nitro compounds. A 100 mL glass autoclave TEM-V100 (TAIATSU TECHNO Corp., Tokyo, Japan), equipped with a mechanical stirrer and a thermocouple, was loaded with 2-octyloxy-5-nitrobenzaldehyde diethyl acetal (5.92 g, 16 mmol), platinum (IV) oxide (0.04 g, 0.18 mmol), and tetrahydrofuran (solvent, 30 mL). The system was then pressurized with hydrogen gas to a constant pressure of 1.0 MPa and left to react for 23 h at room temperature. Following the reaction, the catalyst was removed with filtration through Celite[®]. The filtrate was dried using MgSO_4 and then evaporated to dryness to concentrate the product. The resulting amino-acetal compound was used as a monomer for macrocycle synthesis without further purification. 2-(S)-(-)-(3,7-Dimethyloctyloxy)-5-aminobenzaldehyde diethyl acetal and 2-(2-(2-(2-methoxyethoxy)ethoxy)ethoxy)-5-aminobenzaldehyde diethyl acetal were synthesized according to a similar procedure as mentioned above, except that 2-octyloxy-5-nitrobenzaldehyde diethyl acetal was replaced by 2-(S)-(-)-(3,7-dimethyloctyloxy)-5-nitrobenzaldehyde diethyl acetal for 2-(S)-(-)-(3,7-dimethyloctyloxy)-5-aminobenzaldehyde diethyl acetal, and by 2-(2-(2-(2-methoxyethoxy)ethoxy)ethoxy)-5-nitrobenzaldehyde diethyl acetal for 2-(2-(2-(2-methoxyethoxy)ethoxy)ethoxy)-5-aminobenzaldehyde diethyl acetal.

2.3. Synthesis of Hexakis(2-alkoxy-1,5-phenyleneimine) Macrocycles

2.3.1. Hexakis(2-octyloxy-1,5-phenyleneimine) Macrocycle (OcO-Cm6)

(A) Water Method: A 100 mL sample bottle was filled with 2-octyloxy-5-aminobenzaldehyde diethyl acetal (5.19 g, 16 mmol), tetrahydrofuran (50 mL), and H_2O (1 mL). The mixture was then stirred magnetically at room temperature until precipitates appeared. Yield: 1.73 g (44%). FT-IR (KBr, cm^{-1}): 2925 ($\nu\text{C-H}$, CH_3), 2852 ($\nu\text{C-H}$, CH_2), 1618 ($\nu\text{CH=N}$), 1494, 1253, 1021 (Figure S28). $^1\text{H-NMR}$ (CDCl_3 , δ): 0.83 (t, $J = 7.0$ Hz, 3H, H-15), 1.24 (m, 8H, H-11,12,13,14), 1.48 (quin, $J = 10.4$ Hz, 2H, H-10), 1.81 (quin, $J = 8.0$ Hz, 2H, H-9), 4.02 (t, $J = 6.7$ Hz, 2H, H-8), 6.90 (d, $J = 8.9$ Hz, 1H, H-3), 7.30 (quar, $J = 2.7$ Hz, 1H, H-4), 8.35 (d, $J = 2.7$ Hz, 1H, H-6), 8.98 (s, 1H, H-7). (Figure S29).

(B) AcOH Method: 1 M acetic acid was used instead of water. A 100 mL sample bottle was filled with 2-octyloxy-5-aminobenzaldehyde diethyl acetal (0.89 g, 2.7 mmol), tetrahydrofuran (10 mL), and 1 M acetic acid (1 mL). The mixture was magnetically agitated at room temperature until solid particles began to form. The yield was 0.20 g (44%).

2.3.2. Hexakis(2-((S)-(-)-3,7-dimethyloctyloxy)-1,5-phenyleneimine) Macrocycle ((-)-BCO-Cm6)

A 100 mL glass autoclave container, equipped with a mechanical stirrer and a thermocouple, was filled with 2-((S)-(-)-3,7-dimethyloctyloxy)-5-nitrobenzaldehyde diethyl acetal (3.20 g, 83 mmol), tetrahydrofuran (50 mL), and 5% Pd/C (1.50 g, 0.71 mmol as Pd). Hydrogen gas was introduced into the container at a pressure of 1.0 MPa and catalytic hydrogenation was performed for 20 h. Pd/C was removed using Celite[®] filtration, and

the filtrate was dried with MgSO_4 and evaporated to give 2-((S)-(-)-3,7-dimethyloctyloxy)-5-aminobenzaldehyde diethyl acetal as a yellow liquid. The resulting amino-acetal compound was transferred to a 100 mL sample bottle, and polymerization was initiated under conditions where tetrahydrofuran (20 mL) and H_2O (1 mL) were added, followed by trifluoroacetic acid (0.5 mL) after one week. The polymerization suspension was poured into hexane, and the solid was collected using suction filtration and then washed with tetrahydrofuran. Yield: 0.55 g (18%). FT-IR (KBr, cm^{-1}): 2925 ($\nu\text{C-H}$, CH_3), 2869 ($\nu\text{C-H}$, CH_2), 1623 ($\nu\text{CH=N}$), 1494, 1383, 1364, 1265, 1016 (Figure S30). $^1\text{H-NMR}$ (CDCl_3 , δ): 0.82 (d, $J = 6.7$ Hz, 6H, H-16,17), 0.98 (d, $J = 6.4$ Hz, 3H, H-15), 1.08–1.39 (m, 6H, H-11,12,13), 1.45–1.72 (m, 2H, H-10,14), 1.87–1.93 (m, 2H, H-9), 4.08–4.14 (m, 2H, H-8), 6.98 (d, $J = 8.8$ Hz, 1H, H-3), 7.37 (d, $J = 8.8$ Hz, 1H, H-4), 8.09 (d, $J = 2.7$ Hz, 1H, H-6), 9.05 (s, 1H, H-7) (Figure S31). $^{13}\text{C-NMR}$ (CDCl_3 , δ): 19.8 (C-15), 22.6 (C-17), 22.7 (C-16), 24.7 (C-12), 27.9 (C-14), 30.1 (C-10), 36.2 (C-9), 37.3 (C-11), 39.2 (C-13), 67.4 (C-8), 112.7 (C-6), 125.7 (C-4), 145.8 (C-3), 157.5 (C-7) (Figure S32).

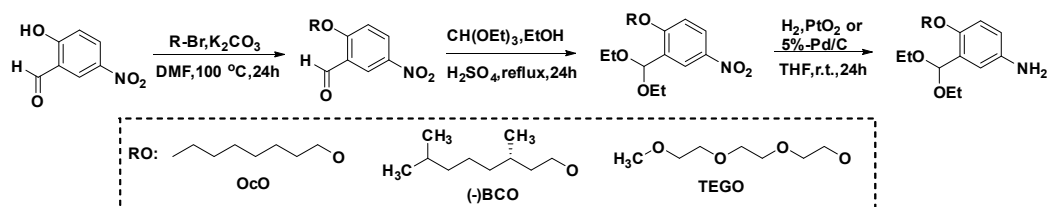
2.3.3. Hexakis(2-(2-(2-(2-methoxyethoxy)ethoxy)ethoxy)-1,5-phenyleneimine) Macrocycle (TEGO-Cm6)

A 100 mL glass autoclave container was filled with 2-(2-(2-(2-methoxyethoxy)ethoxy)ethoxy)-5-nitrobenzaldehyde diethyl acetal (5.25 g, 0.013 mol), tetrahydrofuran (50 mL), and 5% Pd/C (1.53 g, 0.72 mmol as Pd). Catalytic hydrogen reduction was performed for 20 h. The 5% Pd/C was removed using Celite[®] filtration, and, after dehydration with MgSO_4 , the filtrate was evaporated to obtain a reddish-brown liquid. The synthesized product was transferred to a 100 mL sample bottle and polymerization was initiated under conditions where tetrahydrofuran (20 mL) and H_2O (10 mL) were added. After 3 weeks, the solution gelled.

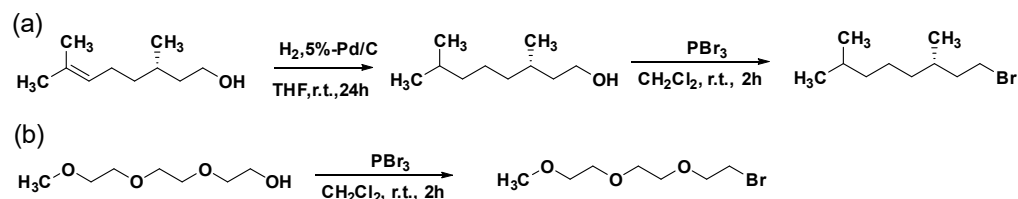
3. Results

3.1. Preparation of Monomers

The synthetic pathway of the monomers (2-alkoxy-5-aminobenzaldehyde diethyl acetals) is illustrated in Scheme 1. 2-Alkoxy-5-nitrobenzaldehydes, including 2-octyloxy-5-nitrobenzaldehyde, 2-((S)-(-)-3,7-dimethyloctyloxy)-5-nitrobenzaldehyde, and 2-(2-(2-(2-methoxyethoxy)ethoxy)ethoxy)-5-nitrobenzaldehyde, were prepared from 2-hydroxy-5-nitrobenzaldehyde and the corresponding 1-bromoalkanes, or its analogue, according to Williamson ether synthesis. (S)-(-)-1-Bromo-3,7-dimethyloctane and 1-bromo-2-(2-(2-methoxyethoxy)ethoxy)ethane were synthesized from (S)-(-)-3,7-dimethyl-6-octen-1-ol and triethylene glycol monomethyl ether, respectively. The synthetic routes involving catalytic hydrogenation and bromination reactions to the bromoalkanes are shown in Scheme 2. The chemical structures of the monomers and their precursors were determined using NMR spectra, and the signals were assigned using DEPT and 2D NMR (H,H-cosy and C,H-cosy) techniques. The spectra are provided in the Supplementary Materials Section as Experimental Procedures and Figures S1–S6.



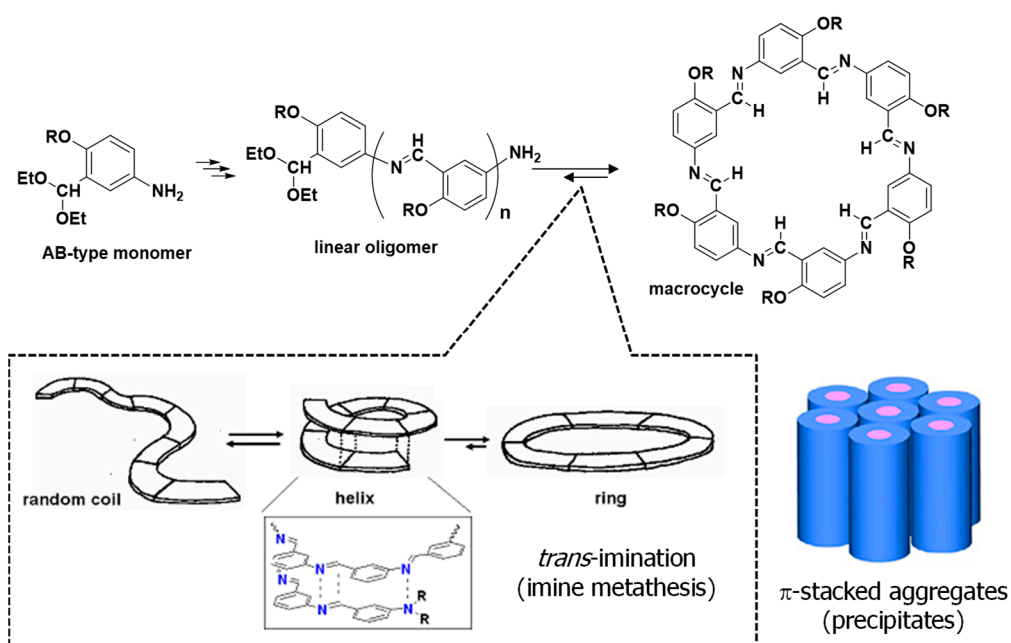
Scheme 1. Synthetic pathway of 2-alkoxy-5-aminobenzaldehyde diethyl acetals. OcO: octyloxy, (-)BCO: (S)-(-)-3,7-dimethyloctyloxy, TEGO: 2-(2-(2-methoxyethoxy)ethoxy)ethoxy.



Scheme 2. Synthesis of (a) (S)-(-)-1-bromo-3,7-dimethyloctane and (b) 1-bromo-2-(2-methoxyethoxy)ethoxyethane.

3.2. Synthesis of Hexakis(2-alkoxy-1,5-phenyleneimine) Macrocycles

Hexakis(2-alkoxy-1,5-phenyleneimine) macrocycles were synthesized using a one-pot procedure where the corresponding acetal-protected AB-type monomers, 2-alkoxy-5-aminobenzaldehyde diethyl acetals, were polycondensated in tetrahydrofuran containing water or acid at room temperature. The general synthetic route of the macrocycle is illustrated in Scheme 3.



Scheme 3. Synthetic route of the macrocycles from 2-alkoxy-5-aminobenzaldehyde diethyl acetals.

The AB-type monomer 2-alkoxy-5-aminobenzaldehyde diethyl acetal, which is protected by an acetal, is gradually deprotected with water or acid. This provides a condensable aldehyde–amino monomer in the polymerization system at a low concentration. These monomers undergo polycondensation to produce linear imine oligomers in a state of equilibrium, as depicted in Scheme 3. A random-coil oligomer forms a helical foldamer with a strong intra-molecular association of hexameric macrocycles that have the same backbone structure. An intra-molecular reaction (*trans*-amination, imine metathesis) takes place between two imine linkages, or between an amino group and a neighboring imine linkage, resulting in a macrocycle [32]. Based on $^1\text{H-NMR}$ analysis of the polymerization solution in Cm6 synthesis [26], it was known that the chain length of the linear oligomer changes to a macrocyclic molecule when it becomes an octamer or larger. Macrocycles that are shape-anisotropic, nearly planar, and persistent are known to aggregate into columnar assemblies in polar solvents, driven by aromatic π -stacking. The macrocycle is stabilized, due to the free energy gained from the intermolecular and noncovalent interactions upon aggregation, making the aggregates the most thermodynamically stable species, and causing them to precipitate [27].

3.2.1. Hexakis(2-octyloxy-1,5-phenyleneimine) Macrocycle (OcO-Cm6)

The macrocycle OcO-Cm6 was produced by the polycondensation of 2-octyloxy-5-aminobenzaldehyde diethyl acetal at room temperature using a mixed solvent of tetrahydrofuran and water (THF/H₂O = 50/1 (v/v)). The MALDI-TOF MASS spectra of the reaction mixture are depicted in Figure 1. In the spectrum of the reaction solution two weeks later (Figure 1a), the peaks corresponding to the unreacted monomer (A1), the dimer (A2), and the macrocycle OcO-Cm6 are observed. After an additional six weeks (totaling two months), the peak of OcO-Cm6 intensifies and becomes the most prominent (Figure 1b).

In order to accelerate the macrocycle formation, 1 M acetic acid (1.0 mL) was used instead of water. The MALDI-TOF MS spectrum of the reaction mixture is illustrated in Figure 2. Despite the short reaction time of one month, a strong peak at 1387.04 m/z, corresponding to the macromolecule OcO-Cm6, appears. It can be seen that AcOH accelerated the deprotection reaction of the acetal group and facilitated the formation of OcO-Cm6. In the FT-IR spectrum of the isolated product, the characteristic peaks were observed at 2925 cm⁻¹ (νC-H, CH₃), 2852 cm⁻¹ (νC-H, CH₂), and 1618 cm⁻¹ (νC=N) (Figure S28). The macrocycle with long alkoxy chains was soluble in specific organic solvents, such as chloroform, whereas Cm6 without side chains was practically insoluble, allowing their structures to be analyzed using NMR. The ¹H-NMR spectrum of hexakis(2-octyloxy-1,5-phenyleneimine) macrocycle (OcO-Cm6) is illustrated in Figure 3. The imine proton signal (H-7) is observed at 8.98 ppm and three phenylene-ring proton signals appear in a range from 6.90 to 8.35 ppm. The proton signal of methylene attached to the oxygen atom in the alkyl side chain (H-8) is observed at 4.02 ppm, and the other protons of the alkyl side chain appear in a range from 0.83 to 1.81 ppm. All the ¹H-NMR signals appear at reasonable positions without excess or deficiency.

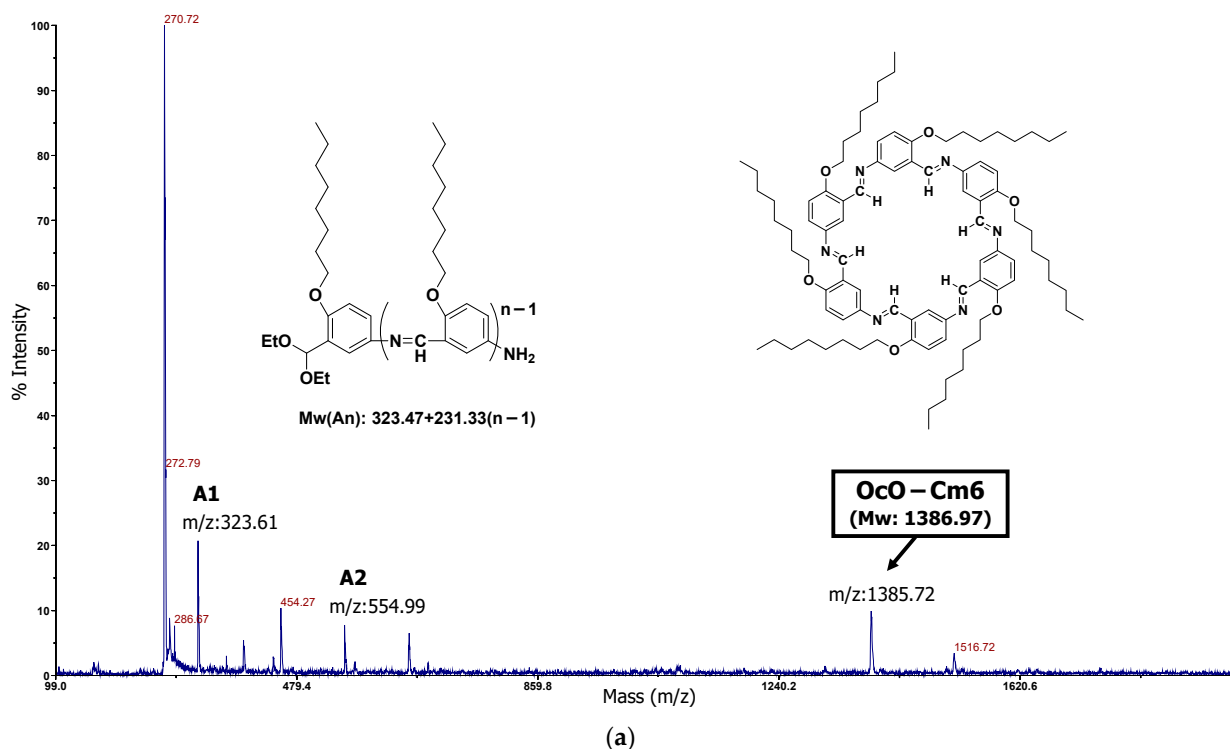


Figure 1. Cont.

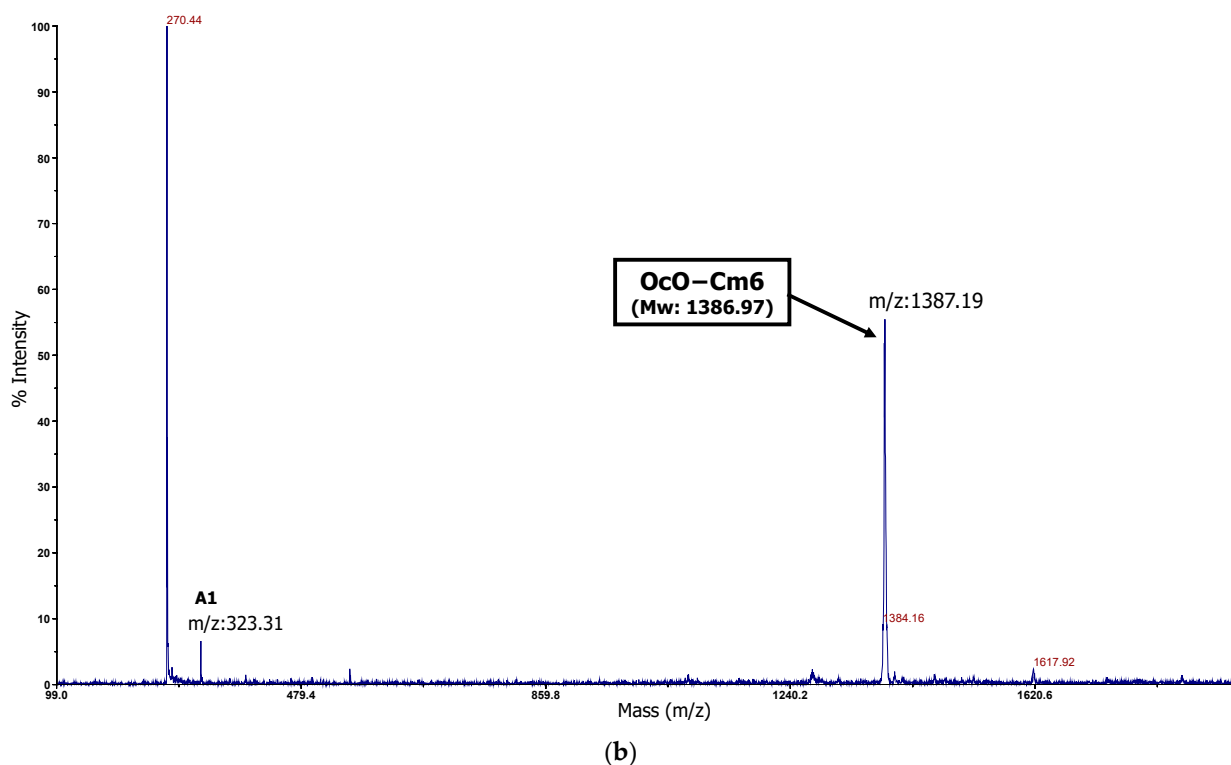


Figure 1. MALDI-TOF MS spectra of reaction mixture: 0.31 M, THF/H₂O = 50/1 (*v/v*), r.t., in air, magnetically stirring. Sampling: (a) two weeks later, homogeneous solution, (b) two months later, suspension containing precipitates.

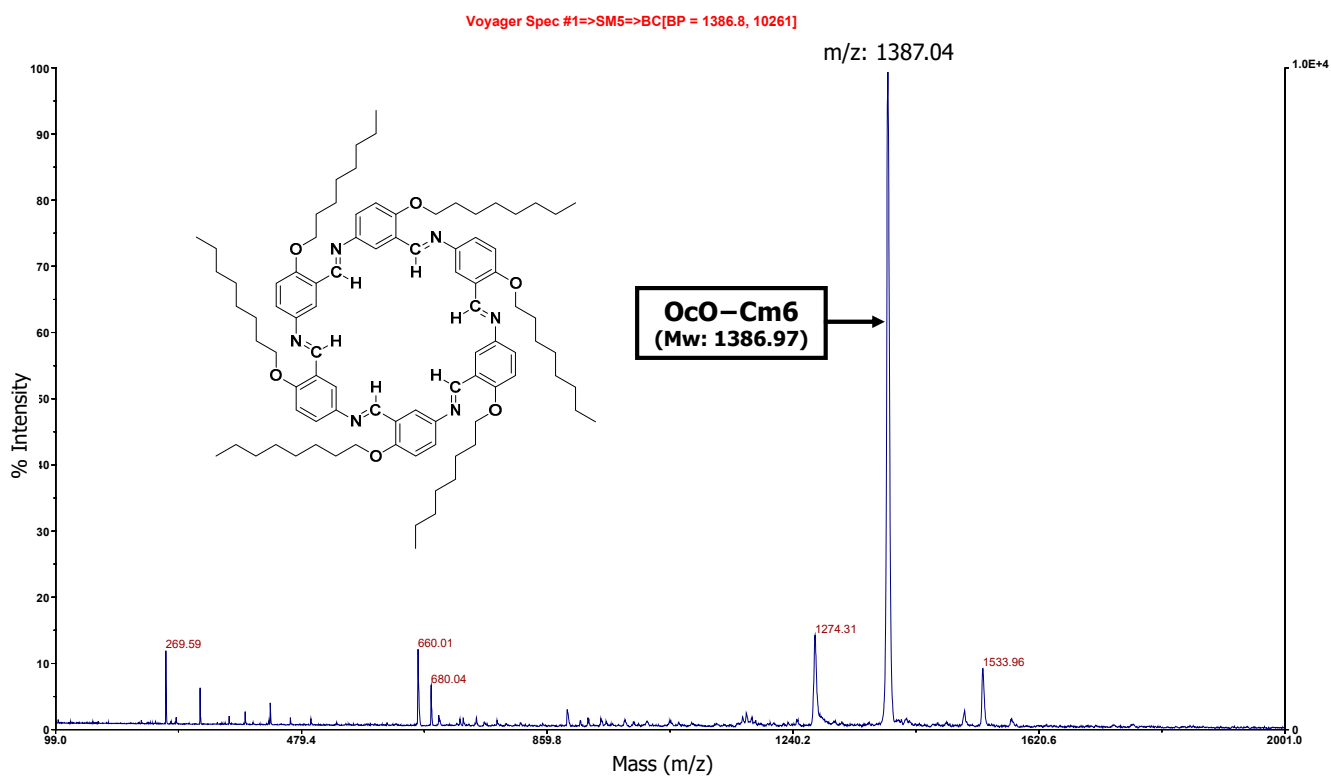


Figure 2. MALDI-TOF MS spectrum of reaction mixture: 0.245 M, THF/AcOH = 50/1 (*v/v*), r.t., in air, magnetically stirring. Sampling: one month later, suspension containing precipitates.

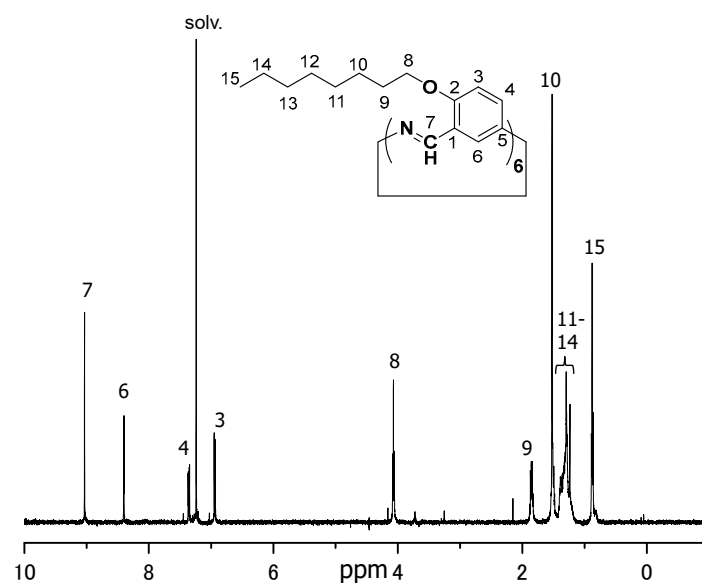


Figure 3. ^1H -NMR spectrum of hexakis(2-octyloxy-1,5-phenyleneimine) macrocycle (OcO-Cm6) in CDCl_3 .

The wide angle X-ray diffraction (WAXD) patterns of finely ground powdered OcO-Cm6 and non-alcoylated Cm6 are illustrated in Figure 4, and the WAXD data (2θ and d value) for OcO-Cm6 are provided in Table 1. The macrocycles exhibit π -stacking, with a separation of 5.5 \AA for OcO-Cm6 and 5.4 \AA for Cm6, and both form a columnar packing with a cylindrical channel. The external diameters for OcO-Cm6 and Cm6 are estimated to be 26.3 \AA and 16.8 \AA , respectively. In the solid state, these columns aggregate to form a hexagonally closest-packed structure.

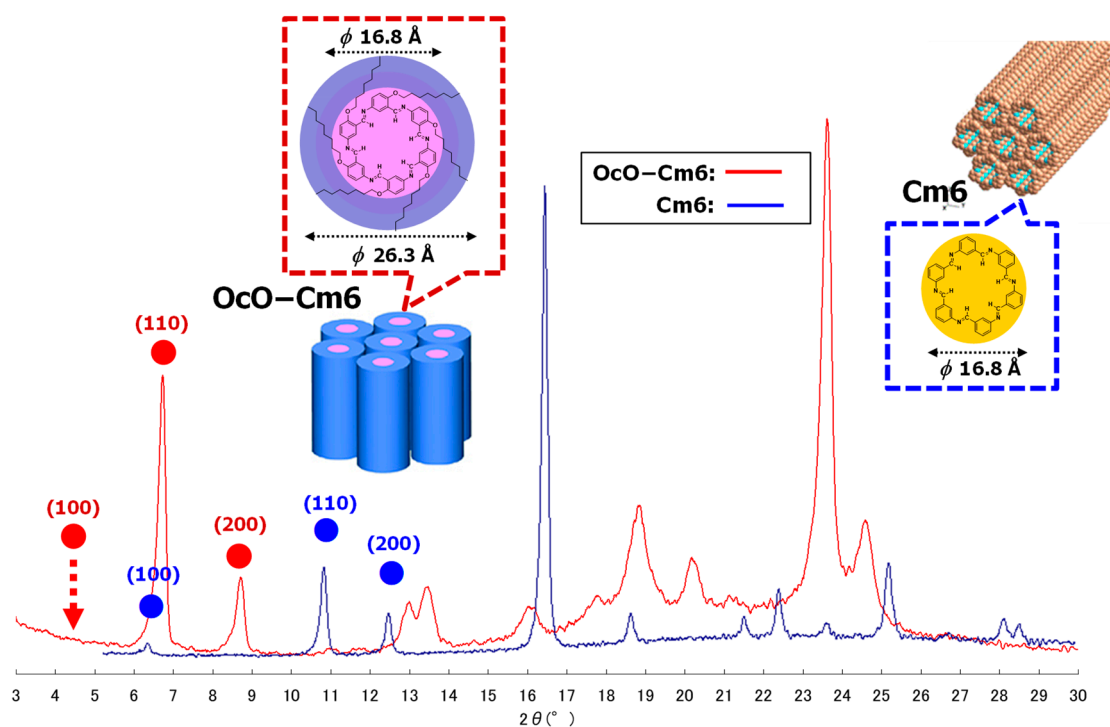


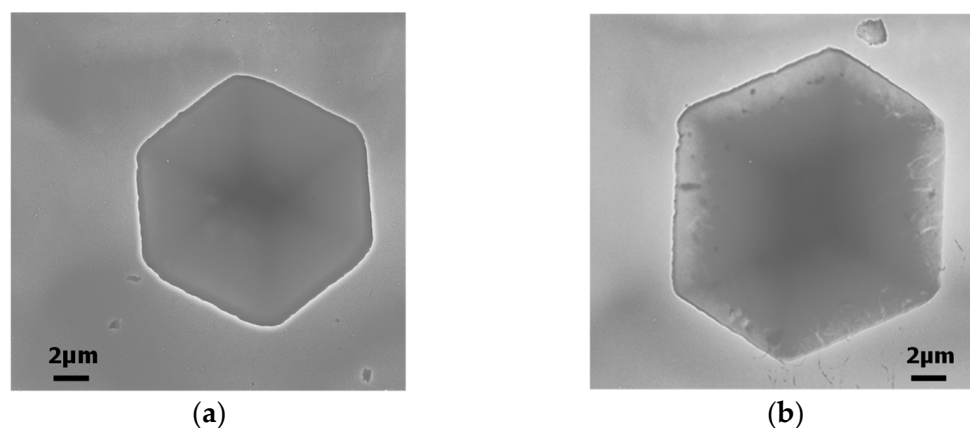
Figure 4. The wide angle X-ray diffraction (WAXD) patterns of hexakis(2-octyloxy-1,5-phenyleneimine) macrocycle (OcO-Cm6) and hexakis(1,5-phenyleneimine) macrocycle (Cm6) [26]. Line color scheme; red: OcO-Cm6, blue: Cm6.

Table 1. The wide angle X-ray diffraction (WAXD) peak data (2θ and d value) of OcO-Cm6.

2θ (deg)	d Value (Å)	2θ (deg)	d Value (Å)
4.35 *	20.29	17.81	4.98
6.73	13.12	18.84	4.71
8.71	10.14	20.17	4.40
12.99	6.81	21.13	4.20
13.47	6.57	23.62	3.76
16.03	5.52	24.59	3.62

* Very weak.

The transmission electron microscopy (TEM) images for OcO-Cm6 can be seen in Figure 5. The two crystals from different locations (Figure 5a,b) are both hexagonal plate-shaped with one side of about 10 μm , and OcO-Cm6 is expected to have hexagonal close-packed nanocolumns that are π -stacked like Cm6 [31], which is consistent with the results of powder X-ray diffraction. However, the crystals were too thick in the (001) direction to measure the electron diffraction (ED).

**Figure 5.** Transmission electron microscopic (TEM) images of hexakis(2-octyloxy-1,5-phenyleneimine) macrocycle (OcO-Cm6) crystals at different locations; (a) hexagonal plate-shaped crystal at a location, (b) that at another location.

The DSC profile of OcO-Cm6 is depicted in Figure 6. Upon heating, small endothermic peaks are observed at 177 $^{\circ}\text{C}$ and 194 $^{\circ}\text{C}$, along with a large endothermic peak at 200 $^{\circ}\text{C}$. During cooling, a significant exothermic peak is observed at 159 $^{\circ}\text{C}$. The DSC measurement results indicate that the melting point (T_m) of OcO-Cm6 is approximately 200 $^{\circ}\text{C}$ and the crystallization temperature (T_c) is around 160 $^{\circ}\text{C}$. Furthermore, the presence of small peaks in addition to T_m and T_c suggests that OcO-Cm6 may be a liquid crystal molecule. The phase transition of OcO-Cm6 was examined using a polarizing microscope with a hot-stage. Upon heating, a phase resembling a mesophase was observed at 190–197 $^{\circ}\text{C}$, transitioning to an isotropic phase above 197 $^{\circ}\text{C}$. During cooling, a phase appearing to be a mesophase was observed at 165–175 $^{\circ}\text{C}$, followed by crystallization at 159 $^{\circ}\text{C}$. Based on these findings, it is proposed that OcO-Cm6 may be an enantiotropic columnar liquid crystal molecule. However, further detailed investigation is required.

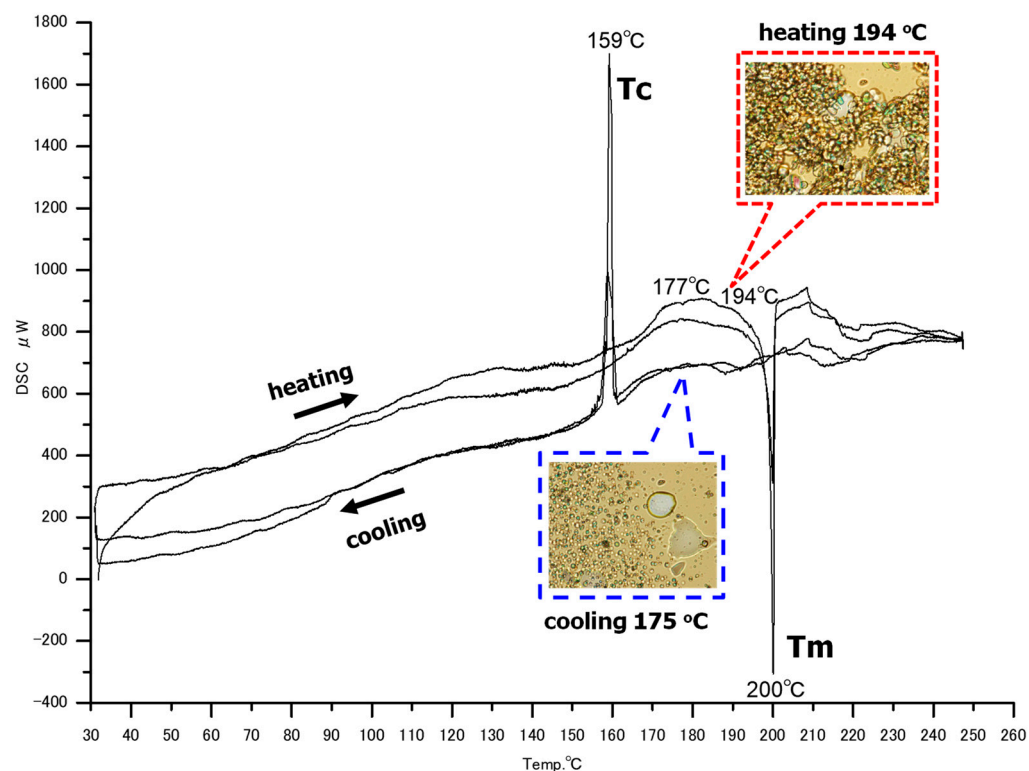


Figure 6. The DSC profile of OcO-Cm6: a heating program from 30°C to 250°C at a heating rate of 1 K/min . The figures within the figure show polarized microscope photographs.

3.2.2. Hexakis(2-((S)-(-)-3,7-dimethyloctyloxy)-1,5-phenyleneimine) Macrocycle ((-)-BCO-Cm6)

2-((S)-(-)-3,7-Dimethyloctyloxy)-5-aminobenzaldehyde diethyl acetal (8.3 mmol) was polymerized in tetrahydrofuran (20 mL) containing water (1.0 mL) at room temperature with magnetic stirring. Water functions to remove the acetal group, thereby restoring the aldehyde group. The polycondensation between the deprotected aldehyde and an amino group of another monomer takes place, and water serves as a catalyst for the polymerization. The reaction process was examined using MALDI-TOF MS spectroscopy. In the MALDI-TOF MS spectrum of the solution one day after the reaction started (Figure 7a) the peaks of the unreacted monomer and the dimer are primarily observed, suggesting that the majority of the acetal groups were not deprotected by water. In order to promote the acetal-deprotection reaction trifluoroacetic acid (0.5 mL) was added to the reaction mixture and allowed to react for an additional two weeks. White precipitates appeared, and the MALDI-TOF MS spectrum of the suspension is shown in Figure 7b, where the peak corresponding to macrocycle ((-)-BCO-Cm6) is observed at 1556.06 (m/z) . The resulting suspension was poured into hexane, and the precipitates were collected, and then washed with tetrahydrofuran (Yield 18%). The spectrum of the isolated product is shown in Figure 7c, in which the intense peak corresponding to ((-)-BCO-Cm6) appears clearly. In the FT-IR spectrum (Figure 7d), characteristic peaks are observed at 2925 cm^{-1} ($\nu\text{C-H, CH}_3$), 2869 cm^{-1} ($\nu\text{C-H, CH}_2$), and 1623 cm^{-1} ($\nu\text{C=N}$).

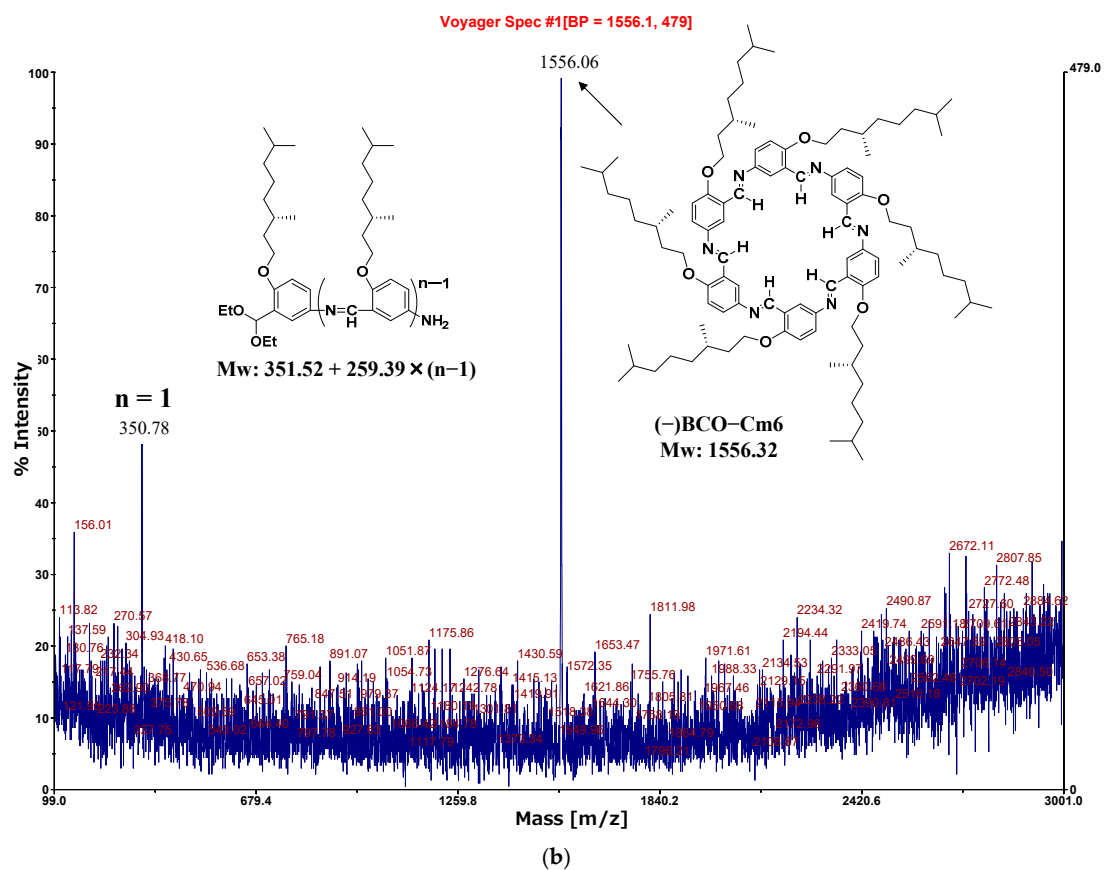
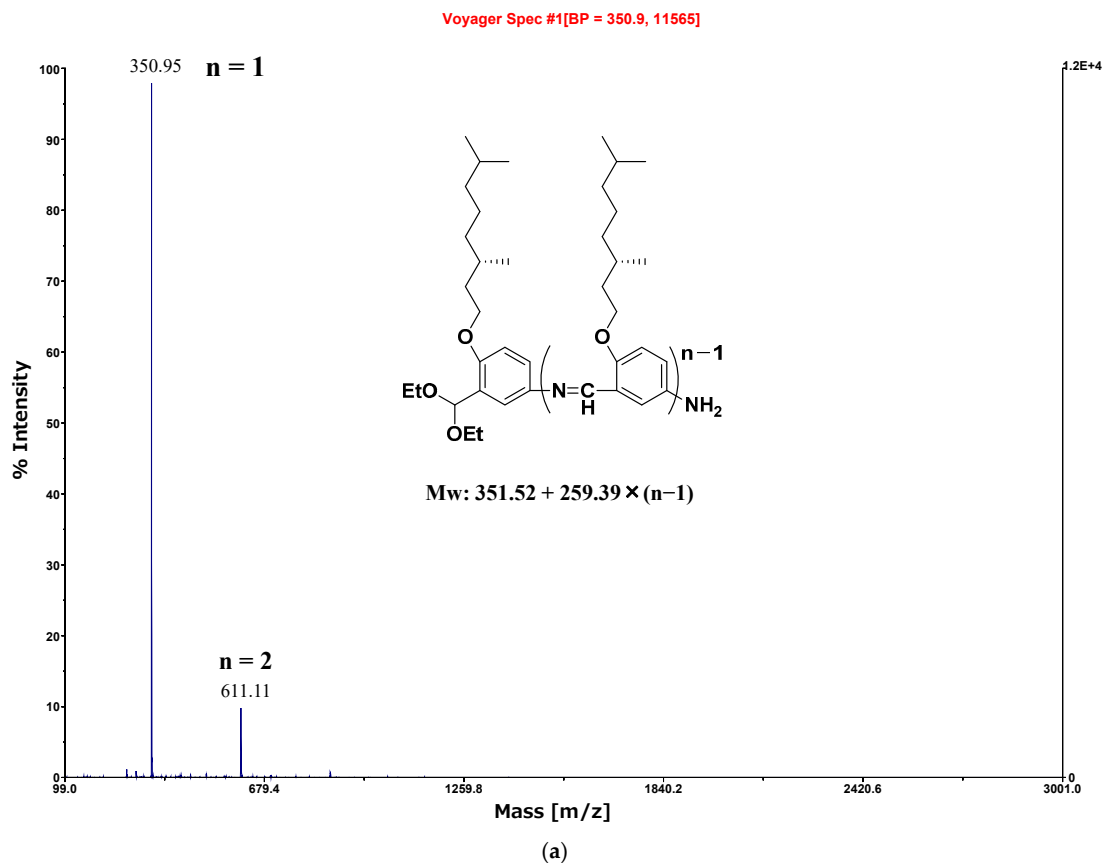


Figure 7. Cont.

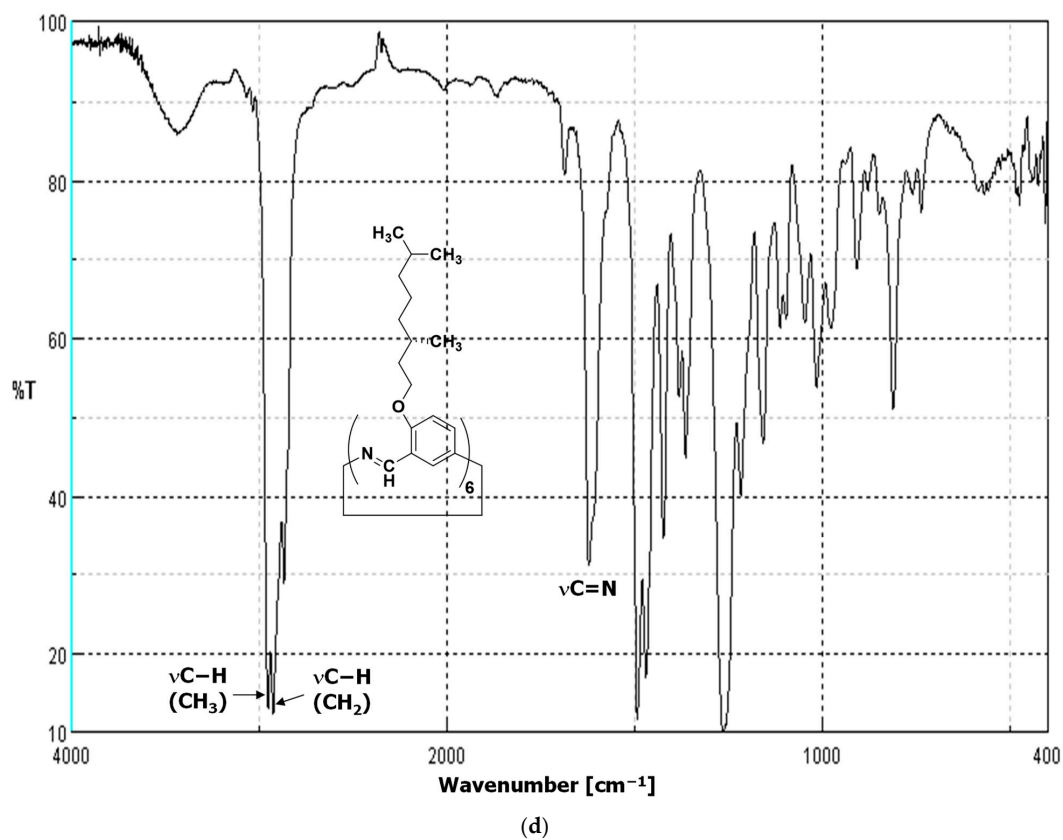
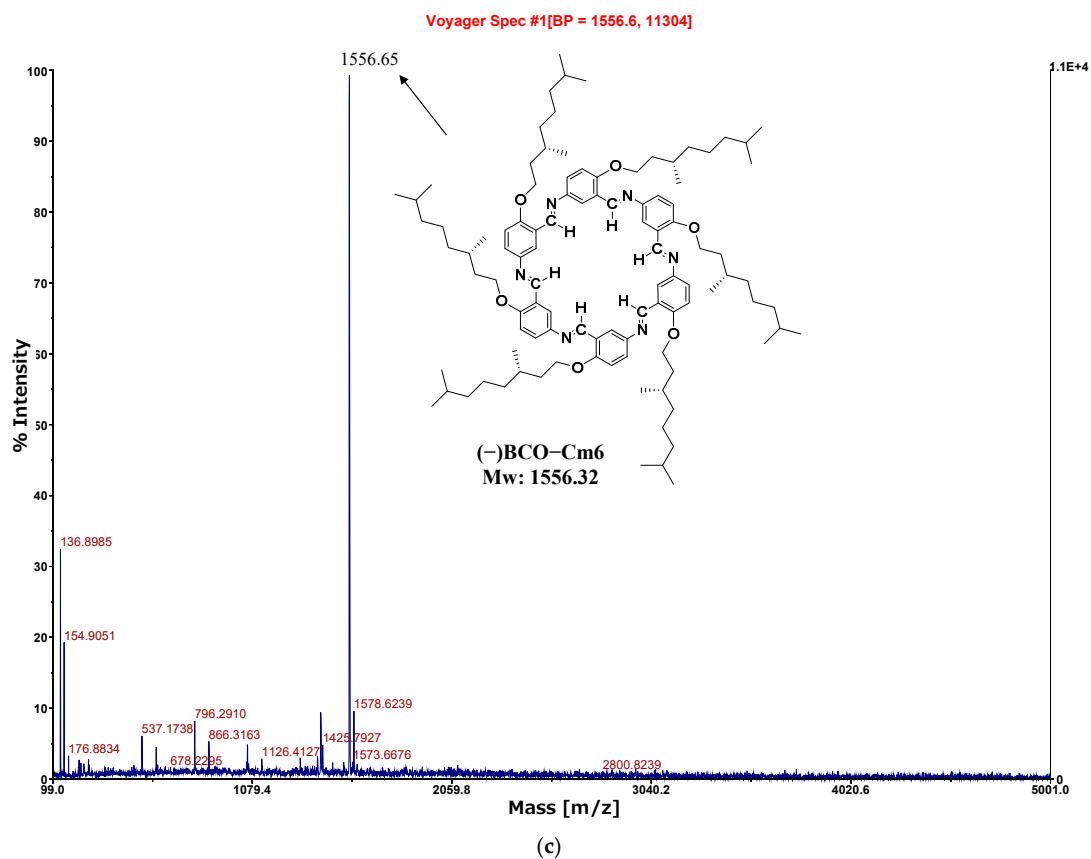


Figure 7. MALDI-TOF MS spectra of the reaction mixture; (a) one day after the reaction start, (b) two weeks after adding trifluoroacetic acid. (c) Isolated precipitates obtained by reprecipitation in hexane. (d) FT-IR spectrum of (-)-BCO-Cm6 powder (KBr, cm^{-1}): 2925 ($\nu\text{C-H}$, CH_3), 2869 ($\nu\text{C-H}$, CH_2), 1623 ($\nu\text{CH=N}$), 1383, 1364, 1494, 1265, 1016.

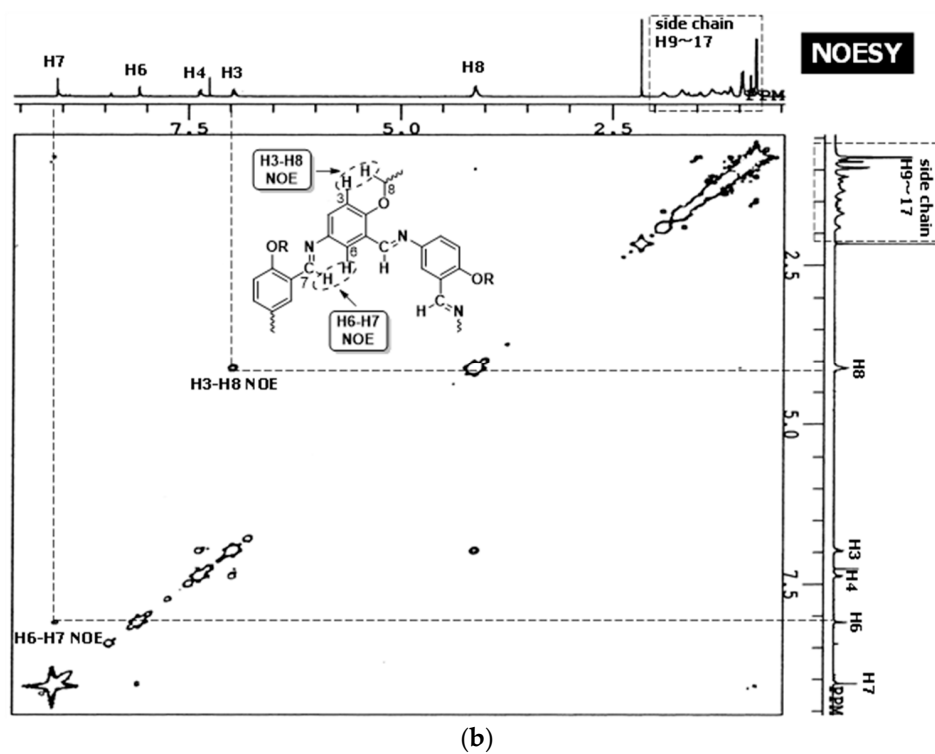


Figure 8. NMR spectra of hexakis(2-((S)-(-)-3,7-dimethyloctyloxy)-1,5-phenyleneimine) (-)BCO-Cm6. (a) $^1\text{H-NMR}$ (CDCl_3 , δ), (b) NOESY (CDCl_3 , δ): cross-peaks of H6–H7 and H3–H8.

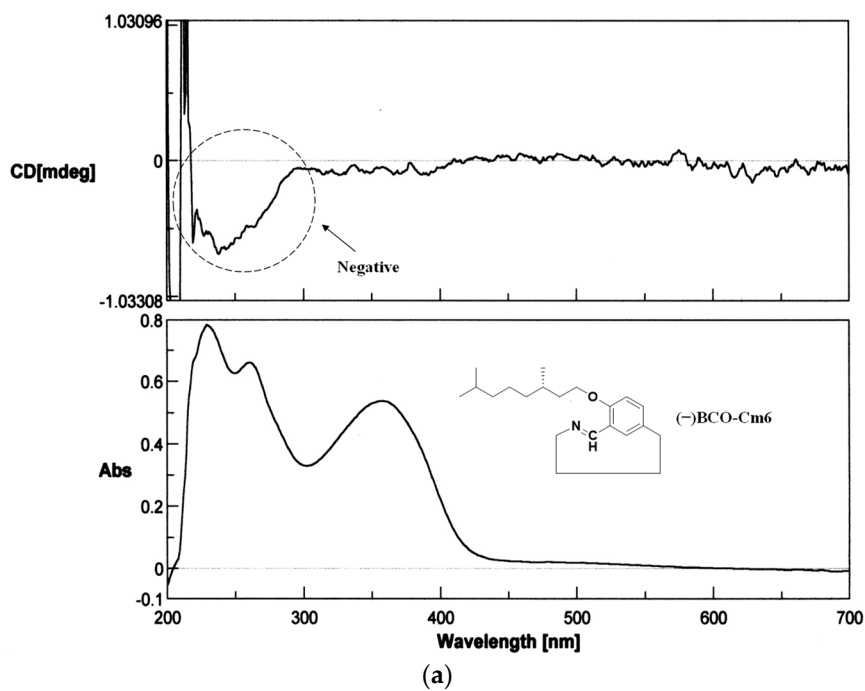


Figure 9. Cont.

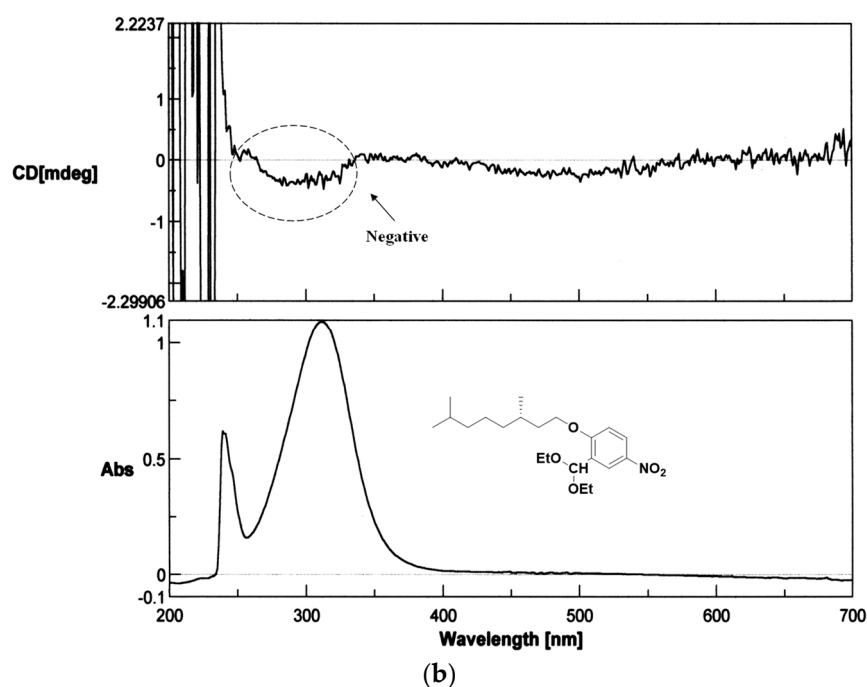


Figure 9. The circular dichroism (CD) spectra of macrocycle (-)BCO-Cm6 and the monomer precursor. 2 mM in chloroform, 0.1 mm cell length. (a) (-)BCO-Cm6, (b) 2-((S)-(-)-3,7-dimethyloctyloxy)-5-nitrobenzaldehyde diethyl acetal.

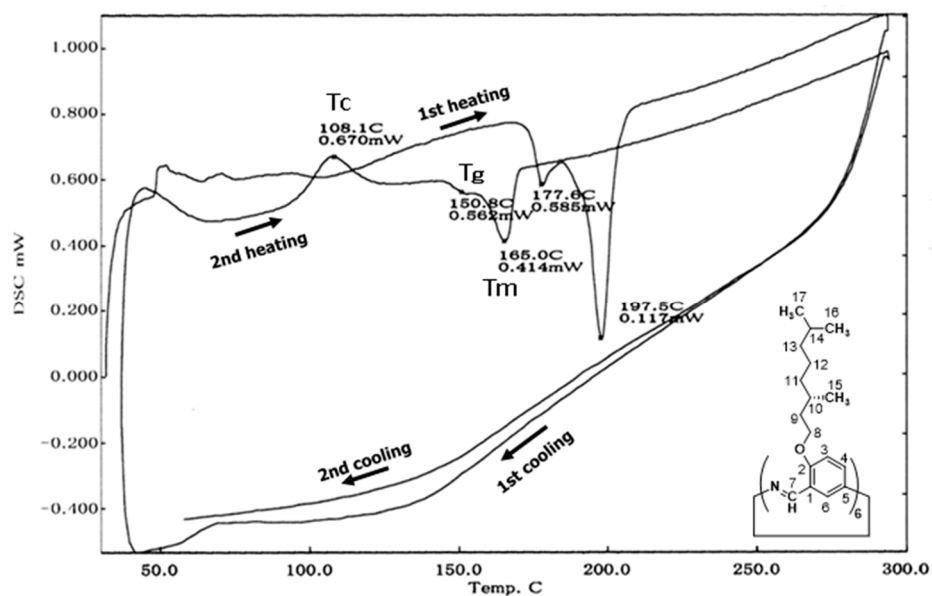


Figure 10. DSC profile of (-)BCO-Cm6 measured in N₂. 1st heating: 30–300 °C, 5 °C/min; 1st cooling: 300–30 °C, 20 °C/min; 2nd heating: 30–300 °C, 5 °C/min; 2nd cooling: 300–30 °C, 20 °C/min.

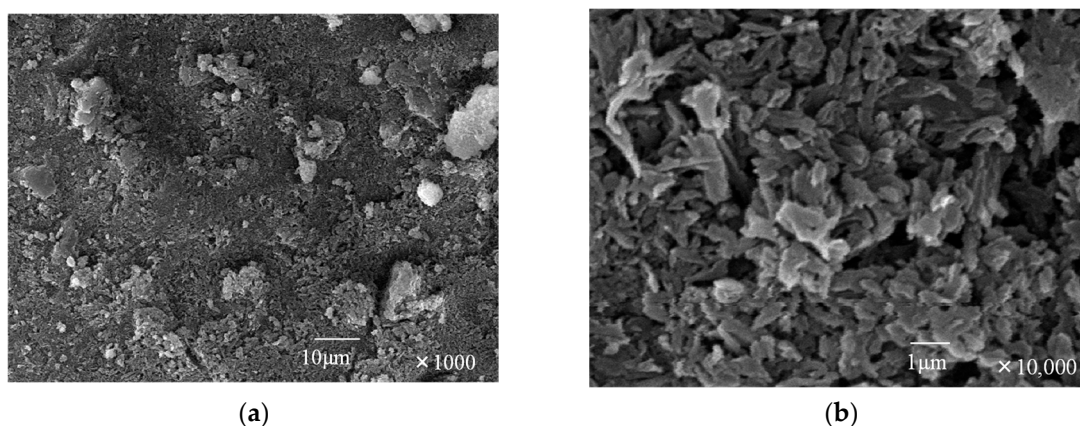


Figure 11. SEM images of (-)BCO-Cm6 powders obtained at magnifications of (a) 1000 and (b) 10,000.

3.2.3. Hexakis(2-(2-(2-methoxyethoxy)ethoxy)ethoxy)-1,5-phenyleneimine) Macrocycle (TEGO-Cm6)

2-(2-(2-Methoxyethoxy)ethoxy)ethoxy-5-aminobenzaldehyde diethyl acetal (13 mmol) was polymerized in tetrahydrofuran (20 mL) containing water (10 mL) at room temperature with magnetic stirring. The polymerization solution gelled after three weeks. The reaction process was examined using MALDI-TOF MS spectroscopy. In the spectrum of the reaction solution (a week later) (Figure 12a), the peaks corresponding to the linear oligomers, which are terminated with an acetal group and an amino group, can be seen. The peak corresponding to macrocycle TEGO-Cm6 appears at 1592.42 m/z in the spectrum of the reaction mixture obtained two weeks later (Figure 12b). After 3 weeks, the solution gelled.

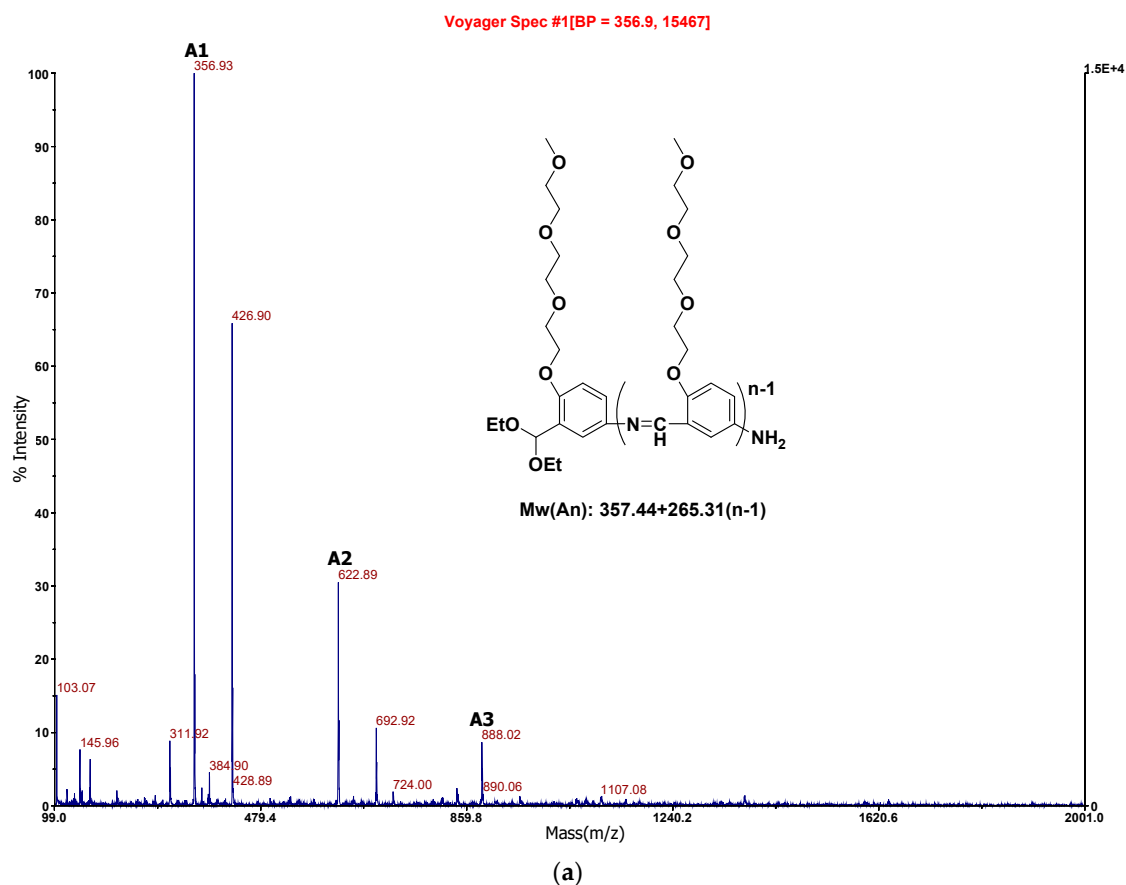


Figure 12. Cont.

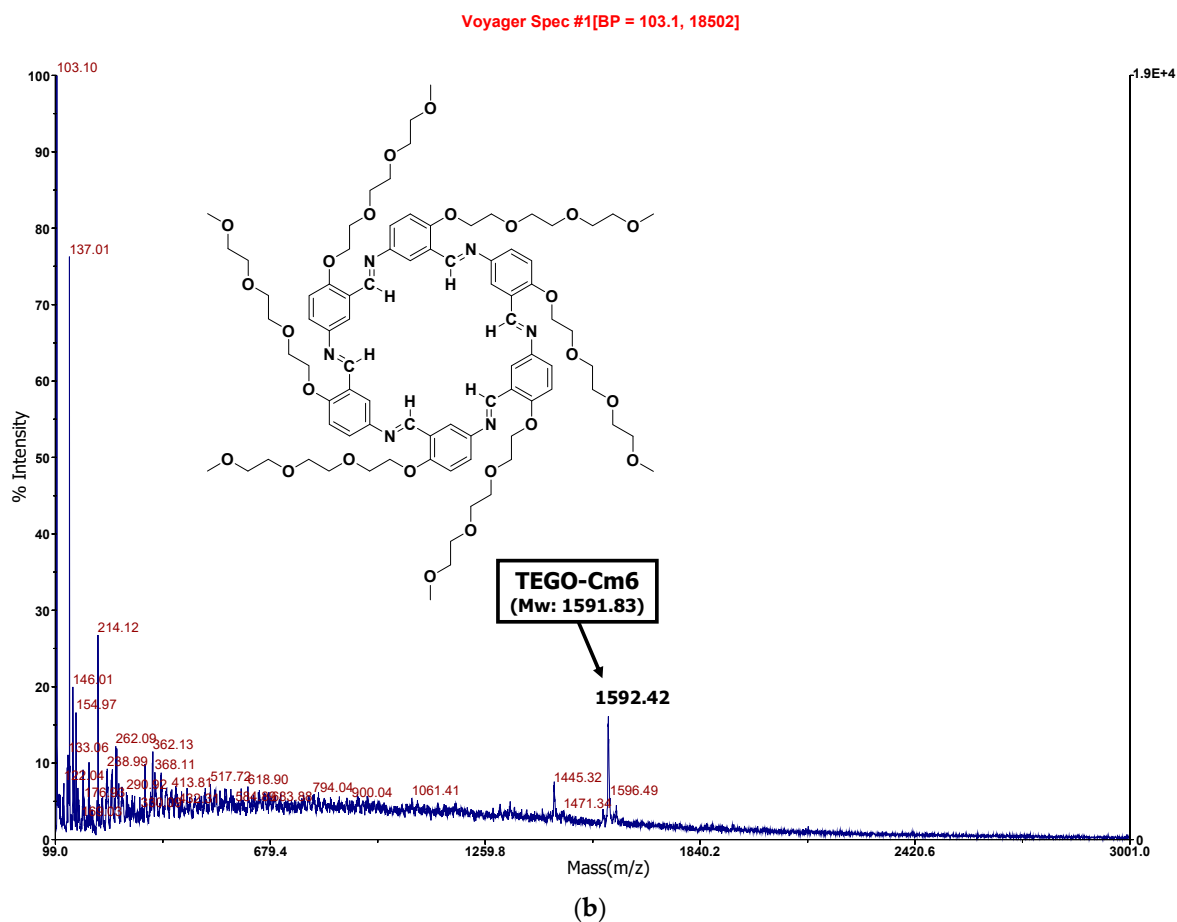


Figure 12. MALDI-TOF MS spectra of reaction mixture: 0.43 M, THF/H₂O = 20/10 (v/v), r.t., in air, magnetically stirring. Sampling: (a) one week later, homogeneous solution; (b) two weeks later, homogeneous solution.

The gel that forms transitions to a liquid state when shaken or subjected to mechanical stress, and reverts to a gel when left undisturbed. In other words, the TEGO-Cm6 hydrogel exhibits thixotropic properties (Figure 13a). Aida, T. et al. reported that a hexa-perihexabenzocoronene (HBC) amphiphile bearing lipophilic dodecyl chains and hydrophilic triethylene glycol chains can self-assemble in THF to form well-defined nanotubes [33]. Similarly, TEGO-Cm6 also forms nanocolumns (nanotubes) in solution, like the aforementioned amphiphilic HBC, and it is suggested that it exhibits thixotropic properties by forming a hydrogen bond network and extending into a fibrous shape (Figure 13b). We hypothesized that the thixotropic phenomenon of the TEGO-Cm6 polymerization solution was influenced by the concentration condition, and examined the relationship between concentration and the gelation phenomenon. Table 2 displays the polymerization conditions and the time when the polymer solution loses its fluidity, as observed visually. Entry 1 gelled on the 20th day after the start of polymerization, but it was not possible to determine whether it exhibited thixotropy due to the small volume of solution. Entries 2 and 3 gelled on the 20th and 24th day after the start of polymerization, respectively, and demonstrated thixotropy. Entry 4 did not gel even after more than 120 days. From these results, it was determined that the thixotropy of this TEGO-Cm6 polymer solution depended on the concentration, and no gelation occurred at low concentration conditions (0.09 mol/L). This result suggested that TEGO-Cm6 could not form a network based on hydrogen bonds, or nanocolumns could not develop into fibrous shapes when the concentration was low.

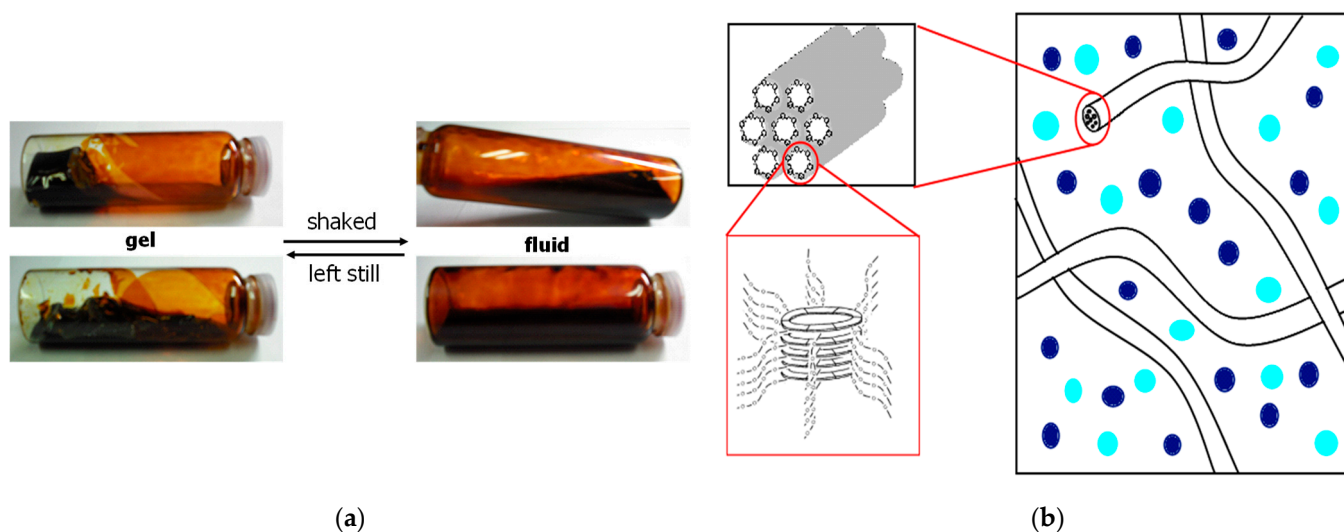


Figure 13. (a) Thixotropic property of the TEGO–Cm6 gel prepared by polycondensation of 2-(2-(2-methoxyethoxy)ethoxy)ethoxy-5-aminobenzaldehyde diethyl acetal (0.43 M) in THF/H₂O at room temperature for three weeks. (b) Imaginary rendering for hydrogel formation by self-assembly of the TEGO–Cm6 yielding nanofibers.

Table 2. The relationship between monomer concentration and gelation time ¹.

Entry	Concentration (mol/L)	Monomer (g)	THF (mL)	H ₂ O (mL)	Gel Time ² (day)
1	0.93	1.00	2.0	1.0	20
2	0.46	5.01	20	10	20
3	0.23	2.51	20	10	24
4	0.09	1.00	20	10	-

¹ Monomer: 2-(2-(2-methoxyethoxy)ethoxy)ethoxy-5-aminobenzaldehyde diethyl acetal, magnetically stirring, room temperature. ² Gelation time: the time when the polymer solution loses its fluidity as observed visually.

4. Conclusions

A simple one-pot synthesis of three types of hexakis(*m*-phenyleneimine) macrocycles with a long alkoxy side chain has been successfully accomplished from acetal-protected AB-type monomers. These monomers were polymerized in tetrahydrofuran containing either water or acid. The presence of acid expedited the deprotection reaction of the acetal group, facilitating the formation of macrocycles. The alkoxyated macrocycles formed nanocolumns through π -stacked self-assembly, and the columns of octyloxyated macrocycle OcO–Cm6 aggregated into a hexagonally closest-packed structure, like Cm6 without the side chain. Oct–Cm6 exhibited an enantiotropic columnar liquid crystal-like mesophase between 165 °C and 197 °C. In the SEM image of (–)BCO–Cm6, columnar substances with diameters ranging from 200 to 300 nm were observed. The polymerization solution for the 2-(2-methoxyethoxy)ethoxyethoxylated macrocycle (TEGO–Cm6) gelled and displayed thixotropic properties by forming a hydrogen bond network and extending in a fibrous shape. No gelation occurred under low monomer-concentration conditions. These thixotropic properties make them ideal candidates for investigation into a range of potential applications, including biomedical smart materials and sensors.

Supplementary Materials: The following supporting information can be downloaded at: <https://www.mdpi.com/article/10.3390/macromol4010001/s1>, Experimental procedures; Scheme S1: Synthesis of 3,7-dimethyloctan-1-ol; Scheme S2: Synthesis of 1-bromo-3,7-dimethyloctane; Scheme S3: Synthesis of 1-bromo-2-(2-(2-methoxyethoxy)ethoxy)ethane; Figure S1: ¹H-NMR spectrum of 3,7-dimethyloctan-1-ol; Figure S2: ¹³C-NMR spectrum of 3,7-dimethyloctan-1-ol; Figure S3: ¹H-NMR spectrum of 1-bromo-3,7-dimethyloctane; Figure S4: ¹³C-NMR spectrum of 1-bromo-3,7-dimethyloctane;

Figure S5: ^1H -NMR spectrum of 1-bromo-2-(2-(2-methoxyethoxy)ethoxy)ethane; Figure S6: ^{13}C -NMR spectrum of 1-bromo-2-(2-(2-methoxyethoxy)ethoxy)ethane; Figure S7: ^1H -NMR spectrum of 2-octyloxy-5-nitrobenzaldehyde; Figure S8: ^{13}C -NMR spectrum of 2-octyloxy-5-nitrobenzaldehyde; Figure S9: ^1H -NMR spectrum of 2-(3,7-dimethyloctyloxy)-5-nitrobenzaldehyde; Figure S10: ^{13}C -NMR spectrum of 2-(3,7-dimethyloctyloxy)-5-nitrobenzaldehyde; Figure S11: ^{13}C -NMR(DEPT-135) spectrum of 2-(3,7-dimethyloctyloxy)-5-nitrobenzaldehyde; Figure S12: H,H-cosy spectrum of 2-(3,7-dimethyloctyloxy)-5-nitrobenzaldehyde; Figure S13: H,H-cosy spectrum of 2-(3,7-dimethyloctyloxy)-5-nitrobenzaldehyde(expanded); Figure S14: C,H-cosy spectrum of 2-(3,7-dimethyloctyloxy)-5-nitrobenzaldehyde; Figure S15: C,H-cosy spectrum of 2-(3,7-dimethyloctyloxy)-5-nitrobenzaldehyde (expanded); Figure S16: ^1H -NMR spectrum of 2-(2-(2-(2-methoxyethoxy)ethoxy)ethoxy)-5-nitrobenzaldehyde; Figure S17: ^{13}C -NMR spectrum of 2-(2-(2-(2-methoxyethoxy)ethoxy)ethoxy)-5-nitrobenzaldehyde; Figure S18: H,H-cosy spectrum of 2-(2-(2-(2-methoxyethoxy)ethoxy)ethoxy)-5-nitrobenzaldehyde; Figure S19: H,H-cosy spectrum of 2-(2-(2-(2-methoxyethoxy)ethoxy)ethoxy)-5-nitrobenzaldehyde (expanded); Figure S20: C,H-cosy spectrum of 2-(2-(2-(2-methoxyethoxy)ethoxy)ethoxy)-5-nitrobenzaldehyde; Figure S21: C,H-cosy spectrum of 2-(2-(2-(2-methoxyethoxy)ethoxy)ethoxy)-5-nitrobenzaldehyde (expanded); Figure S22: ^1H -NMR spectrum of 2-octyloxy-5-nitrobenzaldehyde diethyl acetal; Figure S23: ^{13}C -NMR spectrum of 2-octyloxy-5-nitrobenzaldehyde diethyl acetal; Figure S24: ^1H -NMR spectrum of 2-(3,7-dimethyloctyloxy)-5-nitrobenzaldehyde diethyl acetal; Figure S25: ^{13}C -NMR spectrum of 2-(3,7-dimethyloctyloxy)-5-nitrobenzaldehyde diethyl acetal; Figure S26: ^1H -NMR of 2-(2-(2-(2-methoxyethoxy)ethoxy)ethoxy)-5-nitrobenzaldehyde diethylacetal; Figure S27: ^{13}C -NMR of 2-(2-(2-(2-methoxyethoxy)ethoxy)ethoxy)-5-nitrobenzaldehyde diethylacetal; Figure S28: FT-IR spectrum of hexakis(2-octyloxy-1,5-phenyleneimine) OcO-Cm6; Figure S29: ^1H -NMR spectrum of hexakis(2-octyloxy-1,5-phenyleneimine) macrocycle (OcO-Cm6) in CDCl_3 ; Figure S30: FT-IR spectrum of hexakis(2-((S)-(-)-3,7-dimethyloctyloxy)-1,5-phenyleneimine) macrocycle ((-)-BCO-Cm6); Figure S31: ^1H -NMR spectrum of hexakis(2-((S)-(-)-3,7-dimethyloctyloxy)-1,5-phenyleneimine) macrocycle ((-)-BCO-Cm6) in CDCl_3 ; Figure S32: ^{13}C -NMR spectrum of hexakis(2-((S)-(-)-3,7-dimethyloctyloxy)-1,5-phenyleneimine) macrocycle ((-)-BCO-Cm6) in CDCl_3 .

Funding: This work was supported financially by the Ministry of Education, Culture, Sports, Science and Technology (Japan) Grant-in-Aid for Challenging Exploratory Research. Grant No. 22655037.

Institutional Review Board Statement: Not applicable.

Informed Consent Statement: Not applicable.

Data Availability Statement: The data presented in this study are available upon request from the author.

Acknowledgments: The author thanks Tetsuya Uchida, Okayama University, for TEM-ED measurement. He is also thankful to Kozo Ishida and Seitaro Oishi of Tokyo Polytechnic University for their technical assistance.

Conflicts of Interest: The author declares no conflicts of interest.

References

1. Zhang, W.; Moore, J.S. Shape-persistent macrocycles: Structures and synthetic approaches from arylene and ethynylene building blocks. *Angew. Chem. Int. Ed.* **2006**, *45*, 4416–4439. [[CrossRef](#)] [[PubMed](#)]
2. Jiang, B.; Zhao, M.; Li, S.; Xu, Y.; Loh, T. Macrolide synthesis through intramolecular oxidative cross-coupling of alkenes. *Angew. Chem.* **2018**, *130*, 564–568. [[CrossRef](#)]
3. Kotha, S.; Chavan, S.A.; Shaikh, M. Diversity-oriented approach to macrocyclic cyclophane derivatives by Suzuki–Miyaura cross-coupling and olefin metathesis as key steps. *J. Org. Chem.* **2012**, *77*, 482–489. [[CrossRef](#)] [[PubMed](#)]
4. Zhang, W.; Moore, J.S. Arylene ethynylene macrocycles prepared by precipitation-driven alkyne metathesis. *J. Am. Chem. Soc.* **2004**, *126*, 12796. [[CrossRef](#)]
5. Kotha, S.; Meshram, M.; Dommaraju, Y. Design and synthesis of polycycles, heterocycles, and macrocycles via strategic utilization of ring-closing metathesis. *Chem. Rec.* **2018**, *18*, 1613–1632. [[CrossRef](#)] [[PubMed](#)]
6. Huang, S.; Lei, Z.; Jin, Y.; Zhang, W. By-design molecular architectures via alkyne metathesis. *Chem. Sci.* **2021**, *12*, 9591–9606. [[CrossRef](#)] [[PubMed](#)]
7. Jin, Y.; Zhang, A.; Huang, Y.; Zhang, W. Shape-persistent arylenevinylene macrocycles (AVMs) prepared via acyclic diene metathesis macrocyclization (ADMAC). *Chem. Commun.* **2010**, *46*, 8258–8260. [[CrossRef](#)] [[PubMed](#)]
8. MacLachlan, M.J. Conjugated shape-persistent macrocycles via Schiff-base condensation: New motifs for supramolecular chemistry. *Pure Appl. Chem.* **2006**, *78*, 873–888. [[CrossRef](#)]

9. Lisowski, J. Imine- and amine-type macrocycles derived from chiral diamines and aromatic dianhydrides. *Molecules* **2022**, *27*, 4097. [[CrossRef](#)]
10. He, Z.; Ye, G.; Jiang, W. Imine macrocycle with a deep cavity: Guest-selected formation of syn/anti configuration and guest-controlled reconfiguration. *Chem. A Eur. J.* **2015**, *21*, 3005–3012. [[CrossRef](#)]
11. Zhao, D.; Moore, J.S. Synthesis and self-association of an imine-containing m-phenylene ethynylene macrocycle. *J. Org. Chem.* **2002**, *67*, 3548–3554. [[CrossRef](#)] [[PubMed](#)]
12. Yang, Z.; Esteve, F.; Antheaume, C.; Lehn, J.-M. Dynamic covalent self-assembly and self-sorting processes in the formation of imine-based macrocycles and macrobicyclic cages. *Chem. Sci.* **2023**, *14*, 6631–6642. [[CrossRef](#)] [[PubMed](#)]
13. Chinnaraja, E.; Arunachalam, R.; Pillai, R.S.; Peuronen, A.; Rissanen, K.; Subramanian, P.S. One-pot synthesis of [2+2]-helicite-like macrocycle and 2+4- μ_4 -oxo tetranuclear open frame complexes: Chiroptical properties and asymmetric oxidative coupling of 2-naphthols. *Appl. Organomet. Chem.* **2020**, *34*, e5666. [[CrossRef](#)]
14. Chinnaraja, E.; Arunachalam, R.; Samanta, J.; Natarajan, R.; Subramanian, P.S. Desymmetrization of meso diols using enantiopure zinc (II) dimers: Synthesis and chiroptical properties. *Appl. Organomet. Chem.* **2019**, *33*, e4827. [[CrossRef](#)]
15. Janczak, J.; Prochowicz, D.; Lewiński, J.; Fairen-Jimenez, D.; Bereta, T.; Lisowski, J. Trinuclear cage-like Zn(II) macrocyclic complexes: Enantiomeric recognition and gas adsorption properties. *Chem. Eur. J.* **2016**, *22*, 598–609. [[CrossRef](#)] [[PubMed](#)]
16. Sarnicka, A.; Starynowicz, P.; Lisowski, J. Controlling the macrocycle size by the stoichiometry of the applied template ion. *Chem. Commun.* **2012**, *48*, 2237–2239. [[CrossRef](#)]
17. Byun, J.C.; Lee, N.H.; Mun, D.H.; Park, K.M. Synthesis and characterization of dinuclear copper(II) complexes, $[\text{Cu}_2(\text{[20]-DCHDC}(\text{L}_a)_2)]$ ($\text{L}_a = \text{N}^{3-}$, NCS^- or $\text{S}_2\text{O}_3^{2-}$) with tetraazadiphenol macrocyclic ligand having cyclohexane rings. *Inorg. Chem. Commun.* **2010**, *13*, 1156–1159. [[CrossRef](#)]
18. Gao, J.; Liu, Y.-G.; Zhou, Y.; Boxer, L.M.; Woolley, F.R.; Zingaro, R.A. Artificial Zinc(II) complexes regulate cell cycle and apoptosis-related genes in tumor cell lines. *ChemBioChem* **2007**, *8*, 332–340. [[CrossRef](#)]
19. Gao, J.; Woolley, F.R.; Zingaro, R.A. Catalytic asymmetric cyclopropanation at a chiral platform. *Org. Biomol. Chem.* **2005**, *3*, 2126–2128. [[CrossRef](#)]
20. Gao, J.; Reibenspies, J.H.; Martell, A.E. Structurally defined catalysts for enantioselective oxidative coupling reactions. *Angew. Chem.* **2003**, *115*, 6190–6194. [[CrossRef](#)]
21. Jin, Y.; Wang, Q.; Taynton, P.; Zhang, W. Dynamic covalent chemistry approaches toward macrocycles, molecular cages, and polymers. *Acc. Chem. Res.* **2014**, *47*, 1575–1586. [[CrossRef](#)] [[PubMed](#)]
22. Chao, A.; Negulescu, I.; Zhang, D. Dynamic covalent polymer networks based on degenerative imine bond exchange: Tuning the malleability and self-healing properties by solvent. *Macromolecules* **2016**, *17*, 6277–6284. [[CrossRef](#)]
23. Korich, A.L.; Hughes, T.S. Arylene imine macrocycles of C_{3h} and C_3 symmetry from reductive imination of nitroformylarenes. *Org. Lett.* **2008**, *10*, 5405–5408. [[CrossRef](#)] [[PubMed](#)]
24. Hughes, T.S.; Korich, A.L. Efficient synthesis of an ortho-phenylene-para-phenylene-imine macrocycle. In Proceedings of the 230th ACS National Meeting, Washington, DC, USA, 28 August–1 September 2005. Abstracts of Papers.
25. Moriya, Y.; Yamanaka, M.; Mori, K. Synthesis of C_3 -symmetric macrocyclic triimines from monomers having Boc-protected amine and formyl group. *Chem. Lett.* **2022**, *51*, 217–220. [[CrossRef](#)]
26. Matsumoto, T. Highly efficient one-pot synthesis of hexakis(m-phenyleneimine) macrocycle Cm_6 and the thermostimulated self-healing property through dynamic covalent chemistry. *Polymers* **2023**, *15*, 3542. [[CrossRef](#)] [[PubMed](#)]
27. Seo, S.H.; Jones, T.V.; Seyler, H.; Peters, J.O.; Kim, T.H.; Chang, J.Y.; Tew, G.N. Liquid crystalline order from ortho-phenylene ethynylene macrocycles. *J. Am. Chem. Soc.* **2006**, *128*, 9264–9265. [[CrossRef](#)] [[PubMed](#)]
28. Kawano, S.; Kato, M.; Soumiya, S.; Nakaya, M.; Onoe, J.; Tanaka, K. Columnar liquid crystals from a giant macrocycle mesogen. *Angew. Chem. Int. Ed.* **2017**, *57*, 167–171. [[CrossRef](#)] [[PubMed](#)]
29. Granata, G.; Petralia, S.; Forte, G.; Conoci, S.; Consoli, G.M.L. Injectable supramolecular nanohydrogel from a micellar self-assembling calix[4]arene derivative and curcumin for a sustained drug release. *Mater. Sci. Eng. C* **2020**, *111*, 110842. [[CrossRef](#)]
30. Coh, C.Y.; Mocerino, M.; Ogden, M.I. Macrocyclic gelators. *Supramol. Chem.* **2013**, *25*, 555–566. [[CrossRef](#)]
31. Williamson, A.W. Theory of etherification. *J. Chem. Soc.* **1852**, *4*, 106–112.
32. Zhao, D.; Moore, J.S. Folding-driven reversible polymerization of oligo(m-phenylene ethynylene) imines: Solvent and starter sequence studies. *Macromolecules* **2003**, *36*, 2712–2720. [[CrossRef](#)]
33. Jin, W.; Fukushima, T.; Niki, M.; Aida, T. Self-assembled graphitic nanotubes with one-handed helical arrays of a chiral amphiphilic molecular graphene. *Proc. Natl. Acad. Sci. USA* **2005**, *102*, 10801–10806. [[CrossRef](#)] [[PubMed](#)]

Disclaimer/Publisher's Note: The statements, opinions and data contained in all publications are solely those of the individual author(s) and contributor(s) and not of MDPI and/or the editor(s). MDPI and/or the editor(s) disclaim responsibility for any injury to people or property resulting from any ideas, methods, instructions or products referred to in the content.